

Emergent Braided Matter of Quantum Geometry

Sundance Bilson-Thompson [†], Jonathan Hackett [‡], Louis Kauffman ^{*}, and Yidun Wan [#]

[†] *School of Chemistry and Physics, University of Adelaide
SA 5005, Australia*

[‡] *Perimeter Institute for Theoretical Physics
31 Caroline Street North, Waterloo, ON N2L 2Y5, Canada*

^{*} *Department of Mathematics, University of Illinois at Chicago
851 South Morgan Street, Chicago, Illinois 60607-7045, USA*

[#] *Open Research Centre for Quantum Computing, Kinki University
Kowakae 3-4-1, Higashi-osaka 577-0852, Japan*

August 31, 2011

Abstract. We review and present a few new results of the program of emergent matter as braid excitations of quantum geometry that is represented by braided ribbon networks, which are a generalisation of the spin networks proposed by Penrose and those in models of background independent quantum gravity theories, such as Loop Quantum Gravity and Spin Foam models. This program has been developed in two parallel but complimentary schemes, namely the trivalent and tetravalent schemes. The former studies the trivalent braids on trivalent braided ribbon networks, while the latter investigate the tetravalent braids on tetravalent braided ribbon networks. Both schemes have been fruitful. The trivalent scheme has been quite successful at establishing a correspondence between the trivalent braids and Standard Model particles, whereas the tetravalent scheme has naturally substantiated a rich, dynamical theory of interactions and propagation of tetravalent braids, which is ruled by topological conservation laws. Some recent advances in the program indicate that the two schemes may converge to yield a fundamental theory of matter in quantum spacetime.

Key words: Quantum Gravity, Loop Quantum Gravity, Spin Network, Braided Ribbon Network; Emergent Matter; Braid, Standard Model, Particle Physics, Unification, Braided Tensor Category, Topological Quantum Computation

1 Introduction

1.1 An Invitation to emergent matter of quantum geometry

What is spacetime? What is matter? Physicists and philosophers have pondered these questions for centuries. In fact, an ultimate goal of modern physics is to find a unified answer for both questions. Recently, in order to answer these questions, a novel approach towards emergent¹ matter as topological excitations of quantum geometry has been put forward and extensively developed [1, 2, 3, 4, 5, 6, 7, 8, 9, 10, 11, 12, 13, 14]. Provided with the results of two recent papers[13, 14] along this course, an article that offers a precise review and outlook of this research line seems timely.

A brief historical account is as follows. In 2005, Bilson-Thompson proposed a topological matter model, the Helon model[1], which is based on the preon models of Harari and Shupe[15, 16] and is more elementary than the Standard Model (SM) of particles by interpreting the elementary particles as braids of three ribbons. At the time it was proposed, the Helon Model took the form of a combinatoric game rather than a rigorous theory. In this model, the integral twists of ribbons of braids are interpreted as the quantized electric charges of particles. The permutations of twists on certain braids naturally account for the color charges of quarks and gluons. This model incorporates a simple scheme of the color interaction

¹Here we mean coexisting quantum geometry and matter because our program indicates that a background independent quantum gravity theory may have built-in matter as topological excitations of the quantum geometry described by the theory.

and the electro-weak interaction with lepton and baryon number manifestly conserved. It may also be able to account for the three generations of elementary fermions.

In 2006, Bilson-Thompson, Markopoulou and Smolin[2] coded the Helon Model in certain background independent Quantum Gravity models such as Loop Quantum Gravity (LQG) and Spin Foam (SF) models, by identifying helons with emergent topological excitations of embedded trivalent spin networks that label the states in LQG. Hereafter this will be called the trivalent scheme. Developments of the trivalent scheme[3, 4, 11, 12] allowed the Helon Model to be used as a dictionary between the 3-strand braids of embedded trivalent spin networks and the SM particles. The trivalent scheme led to a new perspective; instead of treating the Helon Model as yet another model of elementary particles, one can encode it in LQG and SF models to make a theory of both spacetime and matter. The dynamics governing particle interactions would then be a consequence of the dynamics of the discrete building blocks of quantum spacetime. In this setting, matter is emergent from quantum spacetime, and the corresponding low energy effective theories may give rise to general relativity coupled with quantum fields.

Unfortunately, results on the stability of braided states[2] in the trivalent scheme strongly suggested that the dynamics of spacetime would allow particle propagation, but not interactions. In effect, braids in the trivalent scheme are “too stable”. To address this issue, and because of the geometrical correspondence between framed 4-valent spin networks and 3-space, a 4-valent scheme was developed[5, 6, 7, 8, 9, 10, 17]. In the 4-valent scheme, the topological structures that can potentially be identified with particles are also 3-strand braids, each of which is formed by the three common edges of two adjacent 4-valent nodes of embedded, framed 4-valent spin networks. The 4-valent scheme gives rise to forms of braid propagation and interaction that are analogous to the dynamics of particles. Nevertheless, the lack of sufficient super-selection rules over an enormous zoo of 3-strand braids in 4-valent scheme withholds a Rosetta Stone that maps the braids to the SM particles. On the other hand, the 4-valent braids may be more elementary, high-energy entities whose low energy limit produces the SM particles[10, 17].

Very recently, two papers by Hackett[13, 14] and work by Bilson-Thompson reported here in Section 4.3, provide a framework that may encode both the trivalent and 4-valent schemes. This would allow the economical reproduction of SM particle states that occurs in the trivalent scheme, and the propagation and interactions that occur in the 4-valent scheme to be combined into a single theory.

As a historical remark, the idea that matter is topological defects of spacetime is an old dream that dates back to 1867 when Lord Kelvin proposed that atoms were knots in ether[18]. Kelvin’s idea failed for its flaws and the limited knowledge people had about our universe then. Nevertheless, this dream has persisted in physicists thereafter. Various proposals of topological matter have arisen as physicists deepen and broaden their recognition of nature. An example is the topological Geon model due to Wheeler and others[19, 20, 21, 22, 23] but the geons therein were unstable and classical. To make stable geons[20], Finkelstein invented the notion of topological conservation laws that also led to advances in condensed matter physics, e.g., topologically conserved excitations in the sine-Gordon theory. Finkelstein’s idea had not been compatible with quantum gravity until the recent work by Markopoulou *et al.*[24, 25, 26] that motivated our work. Analogously, certain condensed matter systems have quasi-particles as collective modes, e.g., phonons and rotons in superfluid He⁴. A recent example in condensed matter physics is a unification scheme due to Wen, *et al.*[27, 28], where gauge theories and linearised gravity appear to be low energy effective descriptions of a new phase, the string-net condensate of lattice spin systems.

In the rest of the Introduction, we briefly introduce concepts and ideas that underpin our approach to emergent matter. We leave main discussions on the trivalent and 4-valent schemes to other sections.

1.2 Noiseless Subsystems

To appreciate the ideas of emergent matter of embedded, framed spin networks, one needs to understand two notions, namely noiseless subsystems and spin networks. Let us address the former first. Noiseless subsystems, put forward in quantum information and computation for quantum error correction[29, 30, 31, 32], are subsets of states of a quantum system that are preserved the evolution algebra of the system,

and hence protected from any error. Markopoulou *et al.* adopted the idea of noiseless subsystems to solve the problem of the low energy limit in background independent quantum gravity theories[25, 33, 34].

Background independence brings in difficulties that retain taking the low energy limit of a background independent theory of quantum gravity[26] as a big open issue, although attempts have been made in various approaches of quantum gravity. In LQG, e.g., [35, 36, 37, 38] use the method of coherent states, which are, according to quantum physics, the quantum states closest to classical ones. For another example, in SF models, [39, 40, 41, 42, 43] utilize n -point correlations functions, which is reasonable because all semiclassical observable are either correlation functions or their derivatives. In view of this, Markopoulou and Kribs[33, 25, 26] proposed a new way to resolve this issue by looking for conserved quantities in background independent theories of gravity. Since the aforementioned noiseless subsystems are conserved states under the evolution algebra of a quantum system, there should be conserved quantities associated with them. This is why one can adapt the method of noiseless subsystems to find conserved quantities of quantum geometry in a large class of background independent theories.

The first application of noiseless subsystems in LQG[34] gives a possible explanation to black hole entropy and how symmetries can emerge from a diffeomorphism invariant formulation of quantum gravity. The noiseless substructures of braided ribbon networks, which appear to encode the helons in models of quantum gravity such as LQG, are braids whose associated conserved quantities are called reduced link invariants[2, 3, 4, 13, 14].

1.3 Spin networks

Penrose invented spin networks as a fundamental discrete description of spacetime[44, 45]; later, Rovelli and Smolin found a more generalized version of spin networks to label the states in LQG Hilbert space[46]. Although the context of spin networks in this article is mainly LQG and its path integral formulation, SF models, it will be clear that our results do not really depend on these models but find their natural home in a generalisation of Penrose's version. Spin networks also arise in lattice gauge theories[47, 48, 49, 50] and topological field theories[51, 52, 53, 54], which are not discussed here.

1.3.1 Penrose's spin networks

Penrose noticed the fundamental incompatibility between General Relativity and Quantum Physics, the problem of the concept of continuum, and the divergences in quantum field theories. He thought that resolving this incompatibility demands a discrete notion of spacetime at the Planck scale, where the classical notion of spacetime is no longer valid. Consequently, the concept of time and space gives way to a more fundamental notion, the microscopic causal relation between quantum events². Knowing that spin (or angular momentum) is intrinsic and characteristic to both quantum systems and classical spacetime, Penrose used combinatoric graphs, consisting of lines intersecting at vertices, to represent the fundamental states of spacetime. Each line in a graph is labeled by a spin, an integer or half integer. Hence, such a graph is called a spin network. Later on, [56] showed that the classical 3-dimensional angles of space can be recovered from trivalent spin networks. Note that these spin networks are unembedded and, opposed to those in LQG, are a direct construction of fundamental quantum spacetime, rather than obtained from quantizing spacetime or General Relativity by any means.

1.3.2 Spin networks from LQG

LQG is a non-perturbative, canonical quantization of General Relativity³. The background independence of General Relativity actually does not leave any room for perturbative quantization[57, 58, 59, 55]. LQG

²The underlying philosophy is relationalism, as opposed to reductionism, reviewed in [59, 62, 55].

³Other non-perturbative approaches to quantum gravity also exist; however, here we focus on LQG.

assumes a $(d + 1)$ -dimensional differential manifold M with a foliation $M = \Sigma \times \mathbb{R}$, without metric but merely a differential structure with a Lie algebra⁴ valued connection 1-form field. We take $d = 3$.

Our approach does not directly depend on any specific techniques and results of LQG but is only inspired by them, so we do not review the technical settings and quantization procedure in LQG.

In LQG, the states are spin networks, which are graphs embedded in Σ (Fig. 1). An edge e is a flux line, labelled by an irreducible representation j_e of a Lie group (usually $SU(2)$ or $SO(3)$). A vertex is labelled by an intertwiner that is the invariant tensor of the labels on the edges meeting at the vertex.

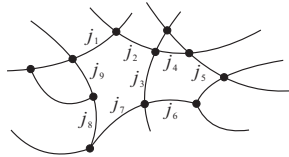


Figure 1: A portion of a generic spin network. Some labels are omitted.

LQG has produced many physical results, which are extensively reviewed in [60, 61, 62]. The result most relevant to this review is the evidence that the space at the Planck scale is discrete because spin network states are eigenstates of operators corresponding to geometric measurements such as area and volume. For example the area operator \hat{A} acting on a 2-dimensional surface S has the spectrum

$$\hat{A}[S]|\Gamma\rangle \propto l_p^2 \sum_{i \in \{\Gamma \cup S\}} \sqrt{j_i(j_i + 1)}|\Gamma\rangle, \quad (1.1)$$

where l_p is the Planck length, and Γ is a spin network that has no vertices on but only edges in S^5 . Likewise, the intertwiners on the nodes of a spin network in a region determine the 3-volume of the region. This fundamental discreteness resolves the singularity problem and also eliminates ultraviolet divergences, as it provides a natural cutoff at the Planck scale to the physical spectrum of the theory.

In general, a vertex of a spin network can have any valence greater than two, the number of edges meeting at the vertex, as seen in Fig. 1. We may consider a basis of spin networks with definite valences, i.e., spin networks respectively with three, four, and higher valences, such that a generic LQG state is a linear combination of these basis states. one may also think that trivalent spin networks may be sufficient to provide a complete basis that spans all spin networks. This is plausible and is suggested by Rovelli[46, 55] for the case of $SU(2)$ and $SO(3)$. The trivalent spin networks represent a basis of LQG state space. That is, associated with a spin network Γ is a state $|\Gamma\rangle$, and for two such states $|\Gamma\rangle$ and $|\Gamma'\rangle$, $\langle \Gamma | \Gamma' \rangle = \delta_{\Gamma \Gamma'}$. Spin network labels on edges and nodes are representations of the group elements, labeling the graphs in the classical configuration space, and the corresponding intertwiners.

Trivalent spin networks have difficulty in representing 3-space because their nodes have zero 3-volume. But each 4-valent node yields a 3-volume⁶[63, 64]. [65] also suggests to carry this correspondence to any higher-valence. In this review, we shall study both trivalent and 4-valent spin networks.

Trivalent spin networks acquire dynamics by evolving under the action of the Hamiltonian constraint operator of LQG, which also helps to realize the 4D diffeomorphism invariance of the theory. The well-accepted form of the Hamiltonian constraint acts only on vertices (Fig. 2)Thiemann[66, 67, 68]; hence, it behaves as a local move that evolves a spin network state to another. In fact, LQG has a path integral formulation, SF models, casting the evolution of spin networks in a systematic, covariant way.

In many studies of SF models[69, 70], spin networks and their histories are unembedded, combinatoric graphs. The key difference between embedded and unembedded spin networks is that the edges in the former can knot, braid, and link. The role of these knots, braids, and links has been a big open

⁴Usually $\mathfrak{su}(2)$ or $\mathfrak{so}(3)$.

⁵If Γ has edges on S , a degeneracy arises and calls for regularization methods to obtain the correct spectrum[55].

⁶This correspondence is at the Planck level. Whether it holds in a continuum limit is still open.

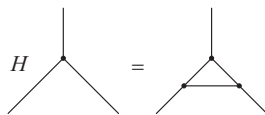


Figure 2: Sketch of of the Hamiltonian constraint acting on a vertex. Irrelevant details are ignored.

issue. Nevertheless, in this article we will show the correspondence between some of these topological structures of embedded spin networks and matter. [71] offers another perspective.

According to SF models[72, 73, 74, 55], trivalent spin networks evolve under two more moves, shown in Fig. 3(a) and (b), including the one in Fig. 2.

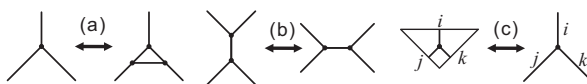


Figure 3: (a): expansion and contraction move. (b): exchange move. (c) a duality.

Trivalent spin networks are the dual skeletons of triangulations of 2D surfaces (Fig. 3(c)), in which a node (an edge) is dual to a triangle (a side of the triangle). This is consistent with 2D because the vertices of trivalent spin networks have zero 3-volume. Hence, the evolution moves of trivalent spin networks are dual to the Pachner moves[75] that relates triangulations of the same surface (Fig. 4). This topological interpretation indicates that summing over histories of the evolution of certain fundamental building blocks produces a quantum spacetime. That is, one can build $(n + 1)$ D spacetime from the evolution of n -valent spin networks. This picture is partly implemented in SF models and fully implemented in another formulation of quantum gravity, Group Field Theories (GFT).

A subtlety exists, however. A spin network with structureless edges and nodes contains less information than an exact dual of a 2D simplicial triangulation, in which two triangles can be glued along a side in two opposite ways. To remedy this, trivalent vertices and their edges should be framed to disks and ribbon respectively (Fig. 4a). We call these (embedded) framed spin networks the **(braided) ribbon networks**⁷. We also name the evolution moves on the (braided) ribbon networks the **adapted Pachner moves** (Fig. 4⁸). The criteria for a legal 2D Pachner move is that the triangles before and after the move

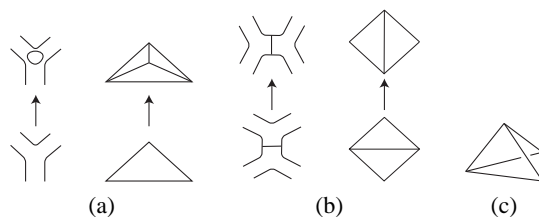


Figure 4: Pachner moves. (a) $1 \rightarrow 3$. (b) $2 \rightarrow 2$.

bounds a 3D tetrahedron (Fig. 4). Interestingly, Major and Smolin[77, 78, 79, 80] suggested that when LQG contains a non-zero cosmological constant, the corresponding spin networks become framed: edges and vertices become ribbons and disks in the trivalent case, and become tubes and spheres in the 4-valent case. We shall loosely call the (embedded) framed 4-valent spin networks the 4-valent (braided) ribbon networks. Likewise, 4-valent ribbon networks evolve under a set of 4-valent adapted dual Pachner moves

⁷For embedded spin networks, the duality is in general only local, i.e., restricted to a single node. This restriction is unnecessary in 2D because a braided ribbon network is dual to a topological manifold globally[76].

⁸This figure is adopted from [11] with the author's permission.

(Section 3.4). Moreover, labels of framed spin networks turn out to be representations of the quantum group, e.g., $SU_q(2)$. In GFT's, the spin networks arise as framed but unembedded.

Our third ansatz requires the embedded 4-valent spin networks to evolve under adapted dual Pachner moves. These moves are adapted and are thus different from those in SF models. In many studies of spin foam models, the spin networks and spin foam histories are taken to be abstract, or unembedded. Our results do not directly apply to these models, as the topological structures our results concern arise from the embedding of the graphs in a topological three manifold. But neither do such models give dynamics for states of loop quantum gravity, which are embedded. A question therefore is how to build spin-foam like dynamics for embedded spin networks. The adapted dual Pachner moves to be defined in Section 3.4 for the 4-valent braided ribbon networks will give an answer.

1.4 Three Ansatzes

All of the above encourages a unification scheme in which matter emerges as topological excitations of the braided ribbon networks. We thus posit that braided ribbon networks are the most fundamental entities of nature⁹, which is beyond LQG and SF Models and actually in accordance with Penrose's original proposal of spin networks, with, however, a great deal of generalization. More precisely, the unification scheme and its results we have obtained are based on three ansatzes:

1. spacetime is pre-geometric and discrete at the fundamental scale.
2. The discrete space is a superposition of basis states represented by braided ribbon networks.
3. The braided ribbon networks evolve under a set of local moves.

These ansatzes are independent of the spacetime dimension. Here, we consider only $(3 + 1)$ -dimensional spacetime, consistent with the observable universe¹⁰. The braided ribbon networks are in general graced with spin network labels, which are otherwise removed in this article because our results obtained so far do not depend on them. The set of local moves include only the adapted dual Pachner moves; however, it may extend to incorporate other moves in future. We hope that classical spacetime would exist as certain limit of the pre-geometric history of the evolution of these graphs.

2 The Trivalent Scheme

The trivalent scheme is the most natural case in which to embed the Helon Model [1], which provides a mapping between braided network states and the fermions and bosons of the SM. Here we will briefly discuss the Helon Model in terms of abstract braided structures, and how those structures may be mapped to particle states and quantities such as hypercharge, baryon number and lepton number. We will then discuss how these braids may be characterised by appropriately chosen topological invariants. At the end of this section we will discuss how such braided structures may be embedded in framed spin networks. The possibility of a unified treatment of trivalent and tetravalent networks is discussed in section 4.3.

2.1 The Helon Model

In the helon model, the subcomponents of SM particles occurring in certain preon models are replaced by a framed braid on three strands. The strands are joined to two surfaces of non-zero size (which we may think of as one disk at each end), and we will suppose there is a way of distinguishing these end

⁹Since all the information due to embedding can be characterized purely combinatorially, to be pointed out later, embedded spin networks (or combinatorial spin networks with embedding data) are more general than the unembedded ones[98, 99].

¹⁰Why our spacetime is $(3+1)$ -dimensional is a big open issue in physics and philosophy. The earliest reasonable argument was due to Ehrenfest in 1917[81] that atoms are instable unless in 3D. Recently, anthropic arguments also arouse. Nevertheless, all these arguments sounds *a posteriori*, and a theory that naturally gives rise to our $(3 + 1)$ spacetime is still missing.

surfaces so that the braids have a “top” and “bottom” (as shown in the left of Fig. 5). For brevity, let us refer to these end surfaces as “caps”. Such a braid (all three strands and the two caps) constitutes a two-dimensional surface and we will immediately restrict our attention to orientable surfaces. The three strands between the caps can in general be distinguished by their relative crossings, and it becomes meaningful to speak of the first, second, and third strand. An entire braid on three strands will represent a single type of fermion or boson.

The individual strands in a braid can carry twists, as mentioned above, and we identify right-handed and left-handed twists as positive and negative electric charges. This is the basis of the name ‘helon’ (evoking the image of a helix) for a single strand. The requirement that we consider only orientable surfaces restricts us to twists that are multiples of 2π , so let us interpret a twist through $\pm 2\pi$ on any helon (that is, any strand) as an electric charge of $\pm e/3$. Twists through $\pm 4\pi$, $\pm 6\pi$, and so on will not be considered, as we shall see below that extra twists can be regarded as equivalent to crossings. Besides the helons carrying twist through -2π and $+2\pi$, there is a third type to consider, carrying no twist. We will denote the three types of helons as H_- , H_+ , and H_0 respectively.

Adapting a scheme originally devised by Harari [15] and Shupe [16], we construct braids composed of three H_+ s (corresponding in electric charge to positrons), three H_- s (corresponding to electrons), a single H_+ and two H_0 s (corresponding to anti-down quarks), a single H_- and two H_0 s (corresponding to down quarks), a single H_0 and two H_+ s (corresponding to up quarks), a single H_0 and two H_- s (corresponding to anti-up quarks), and three H_0 s (corresponding to neutrinos). This scheme reproduces the fermions of the first generation of the SM, with no extra particles. Braids consisting of a mix of H_+ and H_- helons are not allowed when constructing fermions (but are in fact used to construct the gluons). We identify the permutations of braids containing two helons of one type, and one of another (e.g. $H_+H_+H_0$) with the three colour charges of QCD, and write the helons in ordered triplets for convenience (this is, of course, simply notation). The quarks are then as follows (subscripts denote colour);

$$\begin{array}{llll} H_+H_+H_0 & (\overline{u_B}) & H_+H_0H_+ & (\overline{u_G}) & H_0H_+H_+ & (\overline{u_R}) \\ H_0H_0H_+ & (\overline{d_B}) & H_0H_+H_0 & (\overline{d_G}) & H_+H_0H_0 & (\overline{d_R}) \\ H_-H_-H_0 & (\overline{u_B}) & H_-H_0H_- & (\overline{u_G}) & H_0H_-H_- & (\overline{u_R}) \\ H_0H_0H_- & (d_B) & H_0H_-H_0 & (d_G) & H_-H_0H_0 & (d_R). \end{array}$$

while the leptons are;

$$H_+H_+H_+ \quad (e^+) \quad H_0H_0H_0 \quad (\nu_e) \quad H_-H_-H_- \quad (e^-)$$

Note that in this scheme we have identified neutrinos, but not anti-neutrinos. This has occurred because while the H_- may be regarded as the anti-partner to the H_+ , there is no anti-partner to the H_0 helon. This apparent problem will be turned to our advantage in section 2.3.

2.2 Topological invariants of trivalent braids

The braids on three strands may be characterised by an invariant called the *pure twist number*, first described in [12]. This is a triple of real numbers which count the twist remaining on each strand when the braid is deformed such that all crossings are removed. This is possible because any braid on n strands can be written as a product of the generators $\sigma_1, \dots, \sigma_{n-1}$ and their inverses, where σ_i crosses the i^{th} strand in front of the $(i+1)^{\text{th}}$ strand, and σ_i^{-1} crosses the i^{th} strand behind the $(i+1)^{\text{th}}$ strand. The sequence of σ factors defining a braid is called its *braid word*. Clearly, in the case of braids on three strands we are only concerned with σ_1 , σ_2 and their inverses. The generators induce permutations of the strand ordering. The generator σ_1 induces the permutation $P_{1,2}$ (that is, it swaps the 1st and 2nd strands), while the generator σ_2 induces the permutation $P_{2,3}$. Notice also that the same permutation is induced by a generator or its inverse, σ_i^{-1} . Therefore the generators contain more information than the permutations - in particular the direction of the crossing is specified by the generators (as shown in Fig. 5).

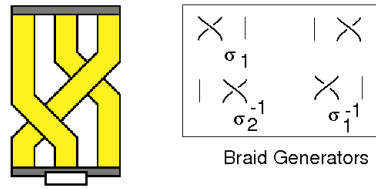


Figure 5: A braid, with the bottom cap denoted by a rectangular block (left) and the generators of the braid group on three strands (right).

It is convenient to define a standardised form for framed braids in which all the twist is isotoped to the top of the braid. Then we can write $[r, s, t]\mathcal{B}$ where \mathcal{B} is an ordinary braid word and $[r, s, t]$ is a triple of multiples of half-integers which catalogue the twists in the ribbons. We shall call this triple of numbers the *twist-word*. Thus a framed braid on three strands is completely specified by the twist word and the braid word. Since these braids are taken to exist on networks embedded in a manifold of three dimensions, we also allow the braids to be deformed such that the top end of the braid is flipped over (effectively feeding it through the strands). This allows us to undo crossings and hence simplify the braid structure, as illustrated in Fig. 6 where we show how a disk with three untwisted ribbons emerging from it (but with two ribbons crossed), can be converted into a disk with uncrossed ribbons and oppositely-directed half-twists in the upper and lower ribbons by flipping the disk over (in the illustration, a negative half-twist in the lower ribbon and positive half-twists in the upper ribbons). In Fig. 7, we show the same process performed on a disk whose (crossed) upper ribbons have been bent downwards to lie besides and to the left of the (initially) lower ribbon. This configuration is nothing other than a framed braid on three strands corresponding to the generator σ_1 (with cap at the bottom omitted). Keeping the ends of the ribbons fixed as before and flipping over the cap so as to remove the crossings now results in three unbraided (i.e. trivially braided) strands, with a positive half-twist on the leftmost strand, a positive half-twist on the middle strand, and a negative half-twist on the rightmost strand. Hence the associated twist-word is $[\frac{1}{2}, \frac{1}{2}, -\frac{1}{2}]$. This illustrates that in the case of braids on three strands, each of the crossing generators can be isotoped to uncrossed strands bearing half-integer twists. By variously bending the top two ribbons down to the right of the bottom ribbon, and/or taking mirror images, and flipping the cap at the top of the braid appropriately we can determine that the generators may be exchanged for twists according to the pattern;

$$\begin{aligned}
 \sigma_1 &\rightarrow \left[\frac{1}{2}, \frac{1}{2}, -\frac{1}{2}\right] \\
 \sigma_1^{-1} &\rightarrow \left[-\frac{1}{2}, -\frac{1}{2}, \frac{1}{2}\right] \\
 \sigma_2 &\rightarrow \left[-\frac{1}{2}, \frac{1}{2}, \frac{1}{2}\right] \\
 \sigma_2^{-1} &\rightarrow \left[\frac{1}{2}, -\frac{1}{2}, -\frac{1}{2}\right]
 \end{aligned}
 \tag{2.1}$$

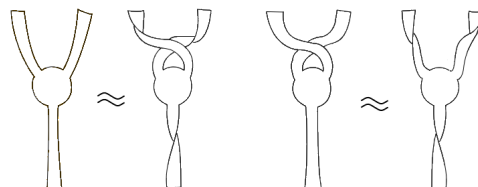


Figure 6: Swapping crossings for twist.

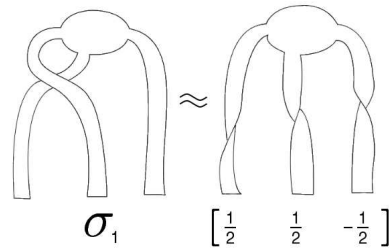


Figure 7: Converting a braid generator into twists.

All braids on three strands can be built up as products of these generators. It should therefore be clear to the reader that we may entirely eliminate the crossings from a braid on three strands. When we do so we uncross the strands one generator at a time (hence permuting them by the permutation P_{σ_i} associated with the crossing σ_i being eliminated) and introduce the twists indicated in equation (2.1). In general, this means that we iterate the process

$$\begin{aligned} [a_1, a_2, a_3][b_1, b_2, b_3]\sigma_i\sigma_j \dots \sigma_m &\rightarrow [a_1 + b_1, a_2 + b_2, a_3 + b_3]\sigma_i\sigma_j \dots \sigma_m \\ &\rightarrow P_{\sigma_i}([a_1 + b_1, a_2 + b_2, a_3 + b_3])[x, y, z]\sigma_j \dots \sigma_m \end{aligned} \quad (2.2)$$

where $[x, y, z]$ is the twist-word associated to σ_i (as listed in equation 2.1, when i is specified), until the braid word becomes the identity.

We shall refer to the form of a braid in which all the crossings have been exchanged for twists as the *pure twist form*. The list of three numbers which characterise the twists on the strands in the pure twist form will be referred to as the *pure twist-word*. The pure twist-word is of interest because it is a topological invariant (since it is obtained when a braid is reduced to a particular simple form i.e. all crossings removed). An algorithm for calculating the pure twist-word of any three-strand braid was described in [12].

One criticism that has been levelled at this research program is that braids appear somewhat ad-hoc and unnatural, however it follows from the discussion above that the use of braids in the Helon Model is a convenience, and that each such braid can be related to a topological invariant which is independent of the way the structure is drawn. When we speak of a particular braid corresponding to a type of fermion, we are therefore simply referring to an equivalence class of topological structures and using one distinctive member of that equivalence class to refer to the entire class. We will see shortly how such general topological structures may be embedded in trivalent spin networks.

2.3 Quantum numbers of particle states

Given the discussion above, it is clear that rotating a diagram of a braid on a page does not change which equivalence class that braid belongs to (and hence we may always perform such a rotation without compromising the validity or usefulness of our model). Let us then pick a certain braid with untwisted strands (i.e. composed entirely of H_0 s) to act as a basic structure for one generation of fermions. Unlike rotation, taking the mirror image of such a braid will produce a member of a different topological equivalence class, in general. Such a braid and its mirror image can be regarded as left-handed and right-handed fermions. By adding one, two, or three twisted strands (H_+ s or H_- s, but not both at the same time), we construct left-handed and right-handed fermions with overall positive and negative charge. This is illustrated in Fig 8. Notice that for any given non-zero magnitude of charge, there are four states (left-handed and right-handed particle, and left-handed and right-handed antiparticle), but for the case of zero charge there exist only two states. We identify these with the neutral left-handed fermion (neutrino) and right-handed fermion (anti-neutrino).

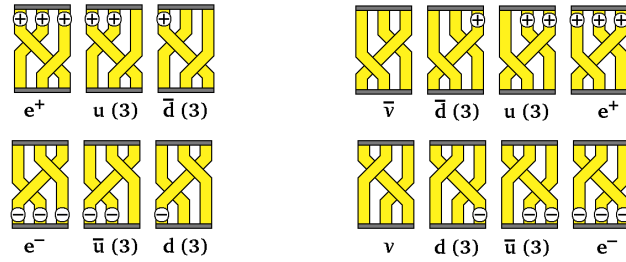


Figure 8: The fermions formed by adding zero, one, two or three charges to a neutral braid. Charged fermions come in two handedness states each, while ν and $\bar{\nu}$ come in only one each. (3) denotes that there are three possible permutations, identified as the quark colours. The bands at top and bottom represent the nodes and connections to the external network (“the rest of the Universe”).

The Helon Model allows us to describe electric charge and colour charge in terms of the topological structure of braids, but we can similarly describe hypercharge and isospin. We begin by assigning a scalar quantity β to braids, such that $\beta = +1$ for the braids on the top row of Figure 8, and $\beta = -1$ to the braids on the bottom row. This effectively distinguishes between fermions with a net positive and net negative charge (and establishes a definition of the equivalent quantity for the neutrinos). Of course β provides only a very crude distinction. To rectify this shortcoming we will define a new quantity, given by one-third the number of “more positive” helons, minus one-third the number of “less positive” helons. We shall denote this quantity by the symbol Ω . To clarify, H_+ helons are considered “more positive” than H_0 helons, which are “more positive” than H_- helons. If $N(H_+)$ is the number of H_+ helons, $N(H_0)$ the number of H_0 s and $N(H_-)$ the number of H_- s within a triplet, and remembering that H_+ and H_- helons never occur within the same braided triplet, we may write

$$\Omega = \beta \left(\frac{1}{3}N(H_+) + \frac{1}{3}N(H_-) - \frac{1}{3}N(H_0) \right). \quad (2.3)$$

Hence we have $\Omega = +1$ for the e^+ , $\Omega = +1/3$ for the u , $\Omega = -1/3$ for the \bar{d} , and $\Omega = -1$ for the anti-neutrino. For the electron, anti-up, down, and neutrino the signs are reversed. With this definition, noting that $N(H_0) = 3 - (N(H_+) + N(H_-))$ and the total electric charge of a fermion is given by

$$Q = \beta \left(\frac{1}{3}N(H_+) + \frac{1}{3}N(H_-) \right), \quad (2.4)$$

it is easy to show that

$$Q = \frac{1}{2}(\beta + \Omega). \quad (2.5)$$

For the quarks and anti-quarks Ω reproduces the SM values of strong hypercharge, while for the leptons β reproduces the SM values of weak hypercharge. We also observe that for quarks $\beta/2$ reproduces the values of the third component of strong isospin, while for leptons $\Omega/2$ reproduces the values of the third component of weak isospin (in short, the roles of β and Ω as isospin and hypercharge are reversed for quarks and leptons). With these correspondences the Gell-Mann–Nishijima relation $Q = I_3 + Y/2$ for quarks may trivially be derived from Eq. (2.5). This construction does not distinguish between left-handed and right-handed fermions, and so it does not match all values of weak isospin and hypercharge in the SM. The reader should remember that the values of isospin and hypercharge in the SM are assigned in an entirely *ad hoc* manner, to reflect the observed asymmetry of the weak interaction, while in the Helon Model these values are constructed. It is possible that with further work the Helon Model may be able to describe (if not explain) the asymmetry of the weak interaction from first principles.

2.4 Interactions and embedding in trivalent networks

Although the Helon Model does not provide a dynamical framework, it is possible to represent the electroweak interactions in a simple manner, by forming the braid product of several braids. The product of two braid diagrams is accomplished by adjoining the strands of the second braid to the corresponding strands of the first braid, as in Fig. 9. The product of two braids, \mathcal{A}_1 and \mathcal{A}_2 , is therefore a single braid, the braid word of which is the concatenation of the generators in the braid words of \mathcal{A}_1 and \mathcal{A}_2 . It therefore follows that if \mathcal{A}_2 is the top-to-bottom mirror image of \mathcal{A}_1 the product of \mathcal{A}_1 and \mathcal{A}_2 will contain no crossings. The reader can easily check that this is true for any braid in the top row of Fig. 8, and the corresponding braid in the bottom row. Such a process suggests particle-antiparticle annihilation. More generally, when the product of two braids is formed, and then decomposed into several braids, the twists on the strands may be shuffled so that the outgoing braids are different from the incoming braids. In this way an interaction such as $u + e^- \rightarrow d + \nu_e$ may be modelled, with the structure of the intermediate braid product suggesting the structure of a boson. A more detailed discussion of how particle interactions can be modelled using braid products is given in [1].

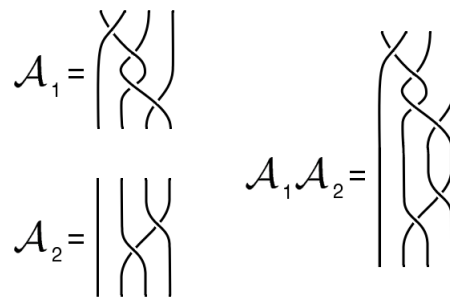


Figure 9: The product of two braids

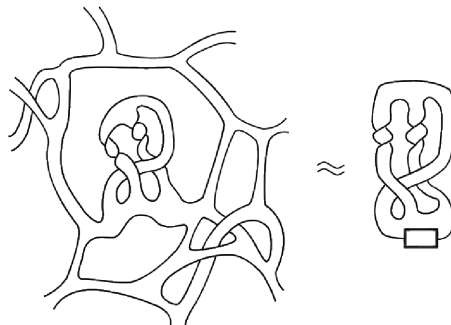


Figure 10: A framed braid on three strands (right), equivalent to a braided substructure in a network (left)

Having established the mapping between braids and SM particles, we now turn to the matter of embedding the Helon Model in trivalent spin networks. In this scheme, a braid occurs as a single node from which three strands (helons) emerge. That is, the cap at the top of a braid is identified as a trivalent node. The strands braid around each other, and then join to the rest of the network at three other nodes (see Figure 10). It was shown in [2] that such embedded braids can be characterised by the linking of the edges of the braid. If we take a diagram of a topological substructure in a trivalent network, and trace along the left and right edges of each strand - discarding any unlinked closed loops - we obtain a diagram of a link corresponding to that structure. This construction is illustrated in Fig. 11. The link obtained may in general be simplified by applying a series of Reidemeister moves to the diagram, to obtain a “reduced link”. The reduced link is an invariant of a braid, so that it does not change no matter

how much the network of nodes and strands is deformed within the manifold in which it is embedded. Likewise, the standard trivalent evolution moves (1-3 expansion move and 2-2 exchange move) do not change the reduced link.

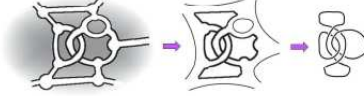


Figure 11: Finding the reduced link of a topological structure within a ribbon network

It is here that the difficulty regarding interactions occurs. In order for any process analogous to the braid product to take place, two braids must be able to combine and then split apart. If the outgoing particle states are to be different from the incoming particle states, then the associated reduced links should also be different. But as noted above, it was shown that this is not possible under the 1-3 and 2-2 evolution moves. While this ensures that individual leptons and quarks will not decay (since the associated reduced link cannot be changed), it also appears to prohibit any non-trivial particle interactions. It is possible that this issue could be addressed by postulating a new evolution move. However in section 4.3 we wish to explore an alternative approach, in which we construct a correspondence between braided networks in the trivalent and tetravalent cases.

3 The 4-valent Scheme

Having seen the results and limitations of the trivalent scheme, we shall move on to the 4-valent scheme, which, although began as an extension to the trivalent one, turned out to be a rich, fully dynamical theory of braids of 4-valent braided ribbon networks. The 4-valent scheme has been studied and cast in two parallel but complementary formalisms, namely the graphic and the algebraic formalisms. While the former offers a more intuitive picture, the latter provides a more convenient playground for theorem-proving and investigating the properties of braids and their dynamics. Consequently, in this Section, we shall adopt the graphic formalism for illustrative purposes only but the algebraic formalism extensively.

3.1 4-valent Braided Ribbon Networks

4-valent braided ribbon networks are framed 4-valent spin networks embedded in \mathbb{R}^3 . The local duality between a node of a 4-valent braided ribbon network and a tetrahedron allows representing a node by a 2-sphere with four circular punctures and its edges by tubes that are welded at the punctures. This is depicted in Fig. 12. We assume that each node is rigid and non-degenerate, such that it can only be translated and rotated, its punctures where its edges are attached are fixed, and no more than two edges of a node are co-planar. Because a tubular edge is dual to a triangular face of a tetrahedron, a tube implicitly carries three racing stripes that record the twist of a tube, which dictates how two tetrahedra are glued on a common face. Section 4 gives a further discussion of the racing stripes.

In a projection, we simplify the tube-sphere notation in Fig. 12(a) to a circle-line notation ((b) or (c)), in which solid lines piercing through the circle represent tubes that are above in the 3D notation, while a dashed line connects two lines as the tubes that are under. There is no information loss in doing so because one can always arrange a node in either the state in Fig. 12(b) or (c) by isotopy before projecting it. Owing to the local duality between a node and a tetrahedron and the symmetry on the latter, if we grab an edge of a node, the other three edges are still on an equal footing, inducing a rotation symmetry w.r.t. the edge being grabbed (Fig. 12(b) & (c)), which will be explained shortly. Therefore, in a projection one can assign states to a node w.r.t. its rotation axis. If the rotation axis is an edge in the back (front), the node is in state \oplus (\ominus) and is called a \oplus -node (\ominus -node), as in Fig. 12(b) ((c)).

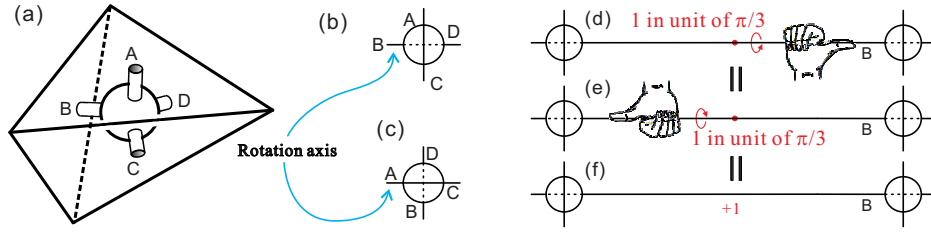


Figure 12: (a) is a tetrahedron and its dual node. In a diagram, a node can have two states, (b) \oplus and (c) \ominus . (f) shows an unambiguous label of the two right-handed $\pi/3$ twists in (d) and (e).

Nonetheless, if the three edges other than the rotation axis of a node must be distinguished, e.g., to be seen shortly in the case of the nodes of a braid, a degeneracy of each state of the node arises. Consider Fig. 12(b), the node is in \oplus w.r.t. edge B ; rotating the node about B produces cyclic permutations of the other edges. Ignoring the twists and crossings that are created by rotations, which will be our next topic, it takes a full rotation for the node to roll back to its original configuration. Among all such permutations, $(C, A, D)^{11}$, (D, C, A) , and (A, D, C) keep the node in \oplus w.r.t. B , whereas (A, C, D) , (C, D, A) , and (D, A, C) flip the node to \ominus . That is, each state has a 3-fold degeneracy; or in other words, each state is a triplet. The six sub-states in total record the full configuration of the node w.r.t. the rotation axis.

If we denote a full rotation by 2π , then the amount of rotation keeping a node within a state triplet is $2\pi/3$; however, a $\pi/3$ causes a node to jump back and forth between two state triplets. Note again that this type of rotations are not the ones with a rigid metric but rather discrete and purely topological. Details of these rotations will be studied in Section 3.3.1.

Naturally, an edges can be twisted discretely. The discussion above of rotations shows that the smallest distinguishable twist is $\pi/3$; higher distinguishable twists in the projection must be integral multiples of $\pi/3$. Fig. 12(d)-(f) shows how the handedness and hence the sign of a twist is unambiguously defined.

3.2 Braids

The graphic notation enables us to find an interesting type of topological excitations of 4-valent braided ribbon networks, namely **3-strand braids** or **4-valent braids**, defined in Fig. 13(a). A 3-strand braid is

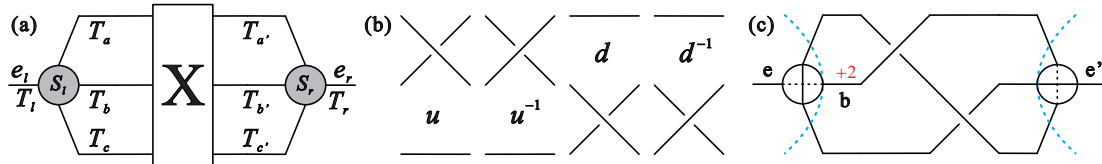


Figure 13: (a) A generic **3-strand braid**. (b) The four generators of X . (c) An example.

made of two **end-nodes** that share three **strands**, which are generically braided and twisted. Each end-node has an **external edge** attached elsewhere in the network. This definition is unambiguous because a braid can always be arranged horizontally as in Fig. 13(a). We disallow the strands of a braid to tangle with any other edges in the network, including the braid's external edges.

A 3-strand braid characterized by an 8-tuple $\{T_l, S_l, T_a, T_b, T_c, X, S_r, T_r\}$ that consists of a pair of end-node states (S_l, S_r) , a pair of **external twists** (T_l, T_r) , a crossing sequence X , and a triple of internal twists (T_a, T_b, T_c) . (S_l, S_r) is valued in $\{+, -\}$. S 's inverse is $-S$ or \bar{S} . X codes the braiding (from left to right) of the three strands; it must be an element in B_3 , the group of ordinary braid of three strands, and is thus generated by the four crossings in Fig. 13(b). All twists are valued in \mathbb{Z} in unit of $\pi/3$.

¹¹In this notation, e.g., (C, A, D) means $C \mapsto A$, $A \mapsto D$, and $D \mapsto C$.

An X of **order** $n = |X|$, the number of crossings, reads $X = x_1 x_2 \cdots x_i \cdots x_n$, where $x_i \in \{u, u^{-1}, d, d^{-1}\}$ is the i -th crossing. We also assign $+1$ or -1 , the crossing number, to each generator according to its handedness, i.e., $u = d = 1$ and $u^{-1} = d^{-1} = -1$. Thus, an x_i is an abstract crossing in a multiplication but $+1$ or -1 in a summation. Suppose X' is a segment of X , then $|X| \geq |X'|$ and three cases exist: Assume $X' = x_1 x_2 \cdots x_n$, 1) if $X = X' x_{n+1} \cdots$, we write $X' \preceq X$, 2) if $X = x_{i_1} x_{i_2} \cdots x_{i_m} X'$, we write $X' \ll X$, and 3) otherwise, we write $X' < X$. X clearly induces a permutation σ_X of the three strands of a braid, which takes value in the permutation group $S_3 = \{\mathbb{1}, (1\ 2), (1\ 3), (2\ 3), (1\ 2\ 3), (1\ 3\ 2)\}$.

σ_X is *left-acting* on the triple of internal twists because it permutes the triple (T_a, T_b, T_c) on the left of the X to the triple $(T_{a'}, T_{b'}, T_{c'})$ on the right by $(T_a, T_b, T_c)\sigma_X = (T_{a'}, T_{b'}, T_{c'})$. Equivalently, we have $(T_a, T_b, T_c) = \sigma_X^{-1}(T_{a'}, T_{b'}, T_{c'})$, where σ_X^{-1} is the inverse of σ_X and is *right-acting*. Besides, $(T_a, T_b, T_c) = (T_d, T_e, T_f)$ means $T_a = T_d$, $T_b = T_e$, and $T_c = T_f$, and we also have $(T_a, T_b, T_c) \pm (T_d, T_e, T_f) = (T_a \pm T_d, T_b \pm T_e, T_c \pm T_f)$. Therefore, A braid can take either of these two algebraic forms,

$$S_T^l[(T_a, T_b, T_c)\sigma_X]_{T_r}^{S_r}, \quad (3.1)$$

$$S_T^l[\sigma_X^{-1}(T_{a'}, T_{b'}, T_{c'})]_{T_r}^{S_r}. \quad (3.2)$$

For instance, the braid in Fig. 13(c) can be written as ${}_0^+[(0, 2, 0)\sigma_{u^{-1}d}]_0^-$ or ${}_0^+[\sigma_{u^{-1}d}^{-1}(2, 0, 0)]_0^-$, where $\sigma_{du^{-1}} = (3\ 1\ 2)$ and $\sigma_{u^{-1}d}^{-1} = (2\ 3\ 1)$. Note that in a braid's expression one should not write the value of σ_X in S_3 explicitly, as σ_X is also responsible for keeping track of X .

We shall see that different types of braids pattern the corresponding 8-tuples differently. For a trivial braid, its X is trivial, and $\sigma_X = \mathbb{1}$; hence, the generic notation uniquely boils down to $S_T^l[T_a, T_b, T_c]_{T_r}^{S_r}$.

Four-valent braids are noiseless topological excitations of braided ribbon networks[24, 2, 26]. We emphasize that 4-valent braids are 3D structures that are better studied in their 2D projections, which are called **braid diagrams** hereafter. In fact, we are dealing with equivalence classes of braids because each braid is equivalent to an infinite number of braids under a set of isotopy moves (to be introduced soon), whose 2D projections relate equivalent braid diagrams. Equivalence classes of braids are in one-to-one correspondence with those of braid diagrams[5, 6, 17]; hence, we need not to distinguish a braid from its diagrams. That is, by a braid we mean all its isotopic braids, and we study this braid by its equivalence class of braid diagrams. In the sequel, we may use braids and braid diagrams interchangeably.

The generators of the X of a 4-valent braid obey the well-known braid relations of B_3 , which are

$$udu^{-1} = d^{-1}ud, \quad u^{-1}du = dud^{-1}, \quad udu = dud \quad (3.3)$$

We assume in any X , these relations have been applied, such that, e.g., $udu^{-1}d^{-1}$ should have been written as $udu^{-1}d^{-1} = d^{-1}udd^{-1} = d^{-1}u$ by the first relation above. This assumption ensures that each 4-valent braid we study has least number of crossings among all the braids related to it by Eq. 3.3. As such, we consider braid diagrams with the same number of crossings and equivalent crossing patterns as the same!

3.3 Equivalence Moves

As aforementioned, equivalent braids and hence equivalent braided ribbon networks are related by a set of local, equivalence moves that act on the nodes and edges of a network without altering the diffeomorphism class of the embedding of the network. One type of these moves are the well-known Reidemeister moves[82], which are translations of nodes and continuous deformation of ribbons[5, 17]. We shall focus on the other type, discrete rotations of nodes, which are peculiar to braided ribbon networks.

3.3.1 $\pi/3$ -Rotations: Generators of rotations

With respect to any of its four edges, a node admits discrete, purely topological rotation symmetries that are not those with a rigid metric and do not affect the diffeomorphism class of the embedding of the node. Section 3.1 points out that each end-nod state is a triplet preserved by a $2\pi/3$ rotation but mapped

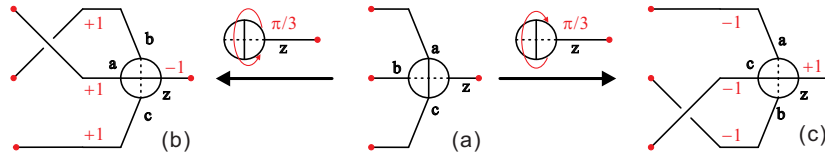


Figure 14: (b) & (c) are results of (a) by rotating the \oplus -node in (a) w.r.t. edge z in two directions respectively. Red dots are assumed connected elsewhere and fixed.

to the other state by a $\pi/3$ rotation. Because two consecutive $\pi/3$ rotations comprise a $2\pi/3$ rotation, $\pi/3$ rotations are generators of all possible discrete rotations of a node w.r.t. an edge of the node. We now show how $\pi/3$ rotations affect a subgraph, in which a node is rotated. In either a \oplus or a \ominus state, a node can be rotated in two opposite directions. Fig. 14 shows the case where a is in a \oplus -state w.r.t. its rotation axis before the $\pi/3$ rotation is done. The effect of a $\pi/3$ rotation on a \ominus -node is the mirror image of Fig. 14. A $\pi/3$ rotation of a node always flips the state of the node, creates a crossing of two edges of the node, and generates a ± 1 on the rotation axis and a ∓ 1 twist on each of the rest three edges.

Since our key topological structures are braids, we wonder how the rotations act on a braid. In this case, e.g., in Fig. 15, we only allow an external edge of a braid to be an rotation axis[5]. In Fig. 15 the left braid is equivalent to the right one with one less crossing. This observation motivates a classification of braids as if they are isolated structures. We name a few important definitions, whose details are referred to [5, 6]. A braid is **reducible** if it is equivalent to a braid with fewer crossings and otherwise **irreducible**. A braid is **left-**, **right-**, or **two-way-reducible** if it can be reduced by rotations on either its left, right, or both end-nodes. A braid equivalent to a trivial braid, i.e., a braid without crossings, is **completely reducible**. The algebraic form of a rotation on a braid as a whole can be found in [8].

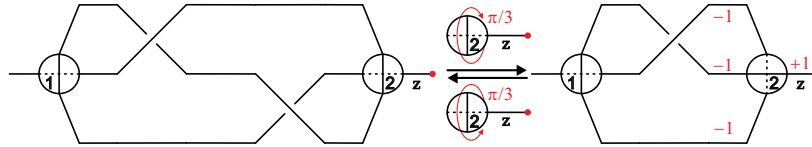


Figure 15: Two braids are equivalent under a $\pi/3$ -rotation of node 2.

As equivalence moves, the rotations and translations should have associated invariants. Although such an invariant exist on arbitrary sub-graph of braided ribbon network, in which equivalence moves act[5, 6], we are more interested in restricting the sub-graphs to be 4-valent braids only. In this case, a braid bears two invariants of discrete rotations, namely its **effective twist** and **effective state**[8],

$$\Theta = T_l + T_r + \sum_{i=a}^c T_i - 2 \sum_{i=1}^{|X|} x_i$$

$$\chi = (-)^{|X|} S_l S_r. \quad (3.4)$$

Moreover, we shall see that both quantities in Eq. 3.4 are also conserved quantities of braid interactions.

3.3.2 Braid Representations

As an equivalence class, a braid should be studied in terms of certain convenient representative of the class. Each braid bears a **unique representation**, in which the braid has twist-free external edges¹². Here is why. Were there two braids with twist-free external edges in one equivalence class, they had

¹²This uniqueness is defined modulo the ordinary braid relations, as explained in Section 3.2.

to be related by rotations, which is contradictory to that any rotation creates twists on an external edge. This representation is convenient to the study of braid dynamics in general.

All irreducible braids in a class must have the same number of crossings; otherwise, the longer ones should either be reducible or belong to another class. Therefore, irreducible braids in a class must have the smallest number of crossings. We henceforth call an irreducible braid an **extremum** of a class. A braid is in an **extremal representation** if it is represented by its extremum. The extremal representation is not unique because a braid has infinite number of extrema[8, 17]. An extremal representation is called a **trivial representation** if the associated extremum has no crossings.

3.4 Dynamics: Evolution Moves

To define the models our results apply to, we have to choose a set of dynamical moves. In SF and other models of spin networks, dual Pachner moves are a common choice[74, 73, 55], as seen in Section 1.3.2 for the trivalent scheme. We now discuss the dual Pachner moves on 4-valent braided ribbon networks.

Let us fix a non-singular topological manifold \mathcal{M} and choose a triangulation of it in terms of tetrahedra embedded in \mathcal{M} whose union is homeomorphic to \mathcal{M} . Any such simplicial triangulation of \mathcal{M} has a natural dual that is a framed 4-valent graph embedded in \mathcal{M} . The framing determines how the tetrahedra are glued on their faces. Thus, a Pachner move on the triangulation should result in a local move in the framed graph, i.e., the dual Pachner move.

Nevertheless, not every embedding of a framed four valent graph in \mathcal{M} is dual to a triangulation of \mathcal{M} . Examples of obstructions to finding the dual include the case of braids (e.g., Figure 13). This is an embedding of a graph that could not have arisen from taking the dual of a regular simplicial triangulation of \mathcal{M} . We note that these obstructions are local, in the sense that a sub-graph of the embedded graph could be cut out and replaced by another sub-graph that would allow the duality to a triangulation of \mathcal{M} .

The question then is how to define the dual Pachner moves on sub-graphs that are not dual to any part of a triangulation of \mathcal{M} . The answer is that we do not. We thus have the basic rule:

*Basic rule:*¹³ The evolution moves on 4-valent braided ribbon networks are the dual Pachner moves that are allowed only on sub-graphs which are dual to a 3-ball.

The Pachner moves and the dual evolution moves that obey the basic rule on the 4-valent braided ribbon networks, namely the $2 \rightarrow 3$ ($3 \rightarrow 2$) and $1 \rightarrow 4$ ($4 \rightarrow 1$) moves, are respectively explained by Fig. 16 and Fig. 17 and their captions. The result of a dual Pachner move is unique up to equivalence

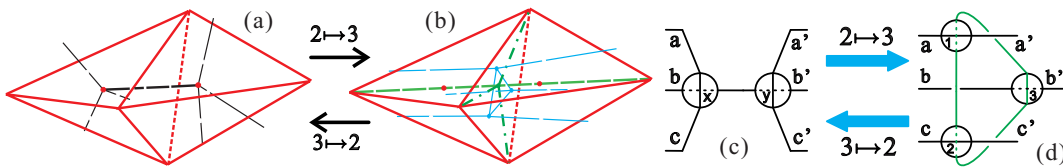


Figure 16: The $2 \leftrightarrow 3$ Pachner moves between (a) two and (b) three tetrahedra. The dual $2 \leftrightarrow 3$ move between (c) two nodes in \oplus -state and (d). (c) and (d) are dual to (a) and (b). The red and dashed green lines in (b) outline the three tetrahedra. Green edges in (d) are generated by the dual $2 \rightarrow 3$ move. If the two nodes in (c) are in \ominus -state, the result of a $2 \rightarrow 3$ move is the left-right mirror image of (d).

moves, i.e., the discrete rotations and adapted Reidemeister moves. The basic rule we posit, which dictates the legitimacy of a dual Pachner move, actually boils down to the following conditions.

Condition 3.1. *A legal dual Pachner move falls into the following three cases.*

1. *Two nodes allow a $2 \rightarrow 3$ move iff they share only one edge and can be put by equivalence moves in the same state with the common edge twist-free (Fig. 16(b) or its mirror image).*

¹³This rule and other possible rules are discussed in detail in [11].

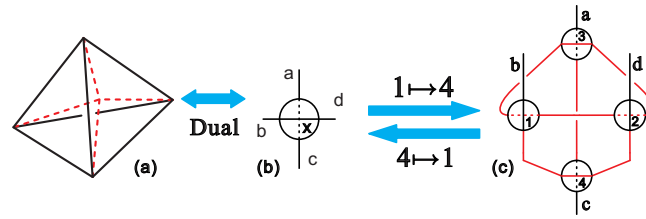


Figure 17: (a) The $1 \leftrightarrow 4$ Pachner moves between one and four tetraheda. The dual $1 \leftrightarrow 4$ moves are between (b) and (c). Red edges in (c) are the generated by the dual $1 \rightarrow 4$ move.

2. Three nodes allow a $3 \rightarrow 2$ move iff they and their edges can be set by equivalence moves as either Fig. 16(c) or its mirror image, where there is a contractible loop made of three twist-free edges.
3. A $1 \rightarrow 4$ move is always doable; however, a $4 \rightarrow 1$ on four nodes is doable iff the four nodes together with their edges can be arranged in the form of either Fig. 17(c) or its mirror image, in which there is a contractible loop and all common edges are twist-free.

In view of Condition 3.1, a $2 \rightarrow 3$ move is illegal on the two end-nodes of the braid in Fig. 13(c), so is a $3 \rightarrow 2$ move on any three nodes that contain this pair, which makes this braid stable under single evolution moves. This generalise to that any nontrivial braid with internal twists is stable under single evolution moves. The **stable braid** are thus considered noiseless subsystems[6] and local excitations with conserved quantities[7, 8]. Section 3.7 has more on the stability and locality of 4-valent braids.

The dual Pachner moves in SF models contain only the permutation relations of edges, which is sufficient only for triangulations. In contrast, our dual Pachner moves are adapted to the embedded case by recording the spatial relation (under or above) of the edges and nodes in a projection of the 3D graph; they are thus called the **adapted dual Pachner moves** and are able to endow embedded 4-valent spin networks a spin-foam like dynamics. This answers the question raised at the end of 1.3.2.

3.5 Dynamics: Propagation, Direct and Exchange Interaction of Braids

In order that the stable braids, as topological excitations of the 4-valent braided ribbon networks, can be candidates for particles or pre-particles, they must be dynamical. Indeed, the evolution moves endow the stable braids rich dynamics: they can propagate and interact. We briefly address braid propagation first.

Since a braid can be considered an insertion in an edge, it makes sense to speak of them propagating to the left or to the right along that edge. To help visualize this in the diagrams we will always arrange a braid so that the edge of the graph it interrupts runs horizontally on the page. There are two types of propagation of braids, namely induced propagation and active propagation.

Under the evolution moves, especially the $1 \leftrightarrow 4$ moves, the ambient network of a braid may expand on one side of a braid but contract on the other side, such that the braid effectively moves towards the side of contraction. We call this phenomenon **induced propagation** because the braid is not directly involved in the evolution and remains the same. Any braid can propagate in this induced way.

Opposed to induced propagation is **active propagation**, which occurs only to specific network configurations and braids; it is called active because the braid's structure undergoes intermediate changes (and probably permanent change of its internal twists) during the propagation. Braids that can propagate in this way are called **actively propagating** and otherwise **stationary** or **non-actively propagating**. Nevertheless, active braid propagation needs some special care that may modify the overall settings of the 4-valent scheme, we thus refer to [6, 17] for details.

Two braids may propagate and meet each other in a situation, such that they can interact. Two interaction types exist: direct interaction and exchange interaction. We shall illustrate these striking behaviours of the braids by figures and present some key results of the dynamics in the algebraic notation.

We first elucidate the direct interaction. In a **direct interaction** of two adjacent braids, one can merge the other, through a sequence of evolution moves. We shall deliver this by a complete example and then by the generalised definition. Fig. 18 depicts all the steps that the two braids in (a) take to become

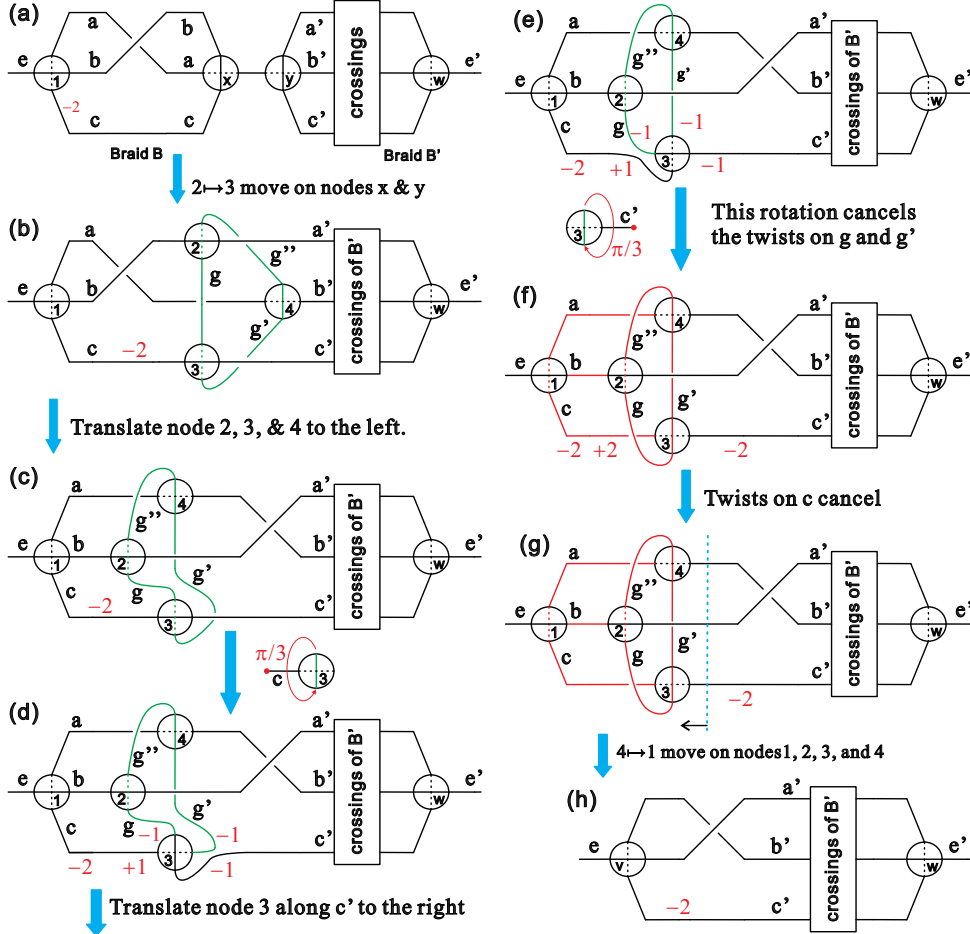


Figure 18: An example of direct right-interaction

the single braid in (h) to complete an interaction. Despite this self-explaining figure, a few remarks are in order. In this example, the equivalence moves - the rotations and translations - are nondynamical but are there only to set the nodes and edges in an proper configuration that manifests the legitimacy of an evolution move, e.g., the final $4 \rightarrow 1$ move (compare it to Fig. 17).

Braid B in Fig. 18(a) is an example of what we call **actively interacting** braids because all the moves are done basically on B 's nodes and edges; B' , except its left end-node, plays no role. Moreover, we Fig. 18 is an example of **direct right-interaction**, in the sense that the actively interacting braid merges with the braid on its right. In fact, a direct interaction always involve at least one actively interacting braid.

For simplicity braid B' is assumed twist-free. One may notice that the twist of -2 on strand c of braid B appears again in the braid in Fig. 18(h). This is not a coincidence but an instance of certain conservation laws that braid interactions follow.

Bearing this example in mind, Fig. 19 serves as an understandable graphical definition of the **direct right-interaction** of two braids. Note that translating the nodes 2, 3, and 4 together with their common edge $g, g',$ and g'' to the left, passing through all of B' 's crossings $X_{B'}$ in Fig. 19 is certainly not always possible because $X_{B'}$ may obstructs the translation by creating a tangle like that in Fig. 19(d). This translation is guaranteed viable only when braid B is at least completely right-reducible (see Fig. 18). Note also that nodes 1, 2, 3, and 4 with their edges cannot always be arranged by equivalence moves to

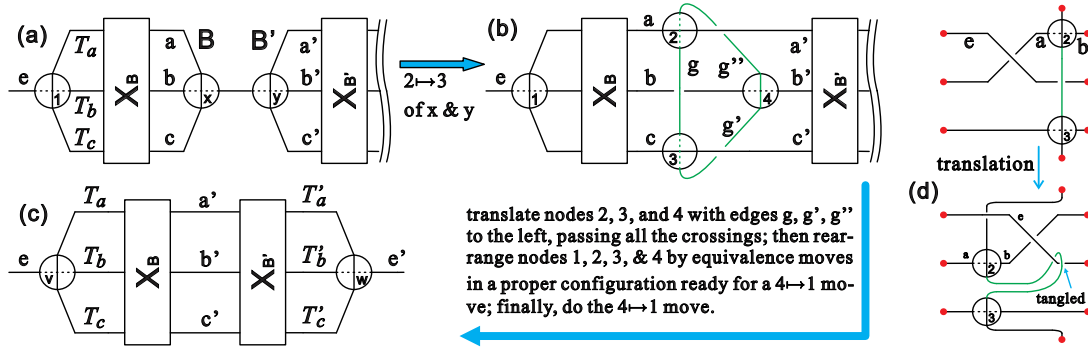
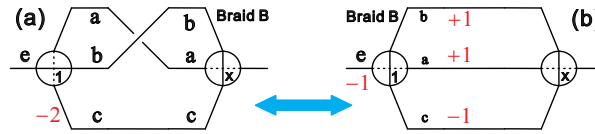


Figure 19: (a)-(c) Definition of the direct right-interaction. (d) An obstructed translation.

meet Condition 3.1(3), such that the final $4 \rightarrow 1$ move can be done to complete the interaction. If all steps in Fig. 19 are possible, braid B must be actively interacting.

It is a theorem[6, 7] that a braid is actively interacting constrains the braid to be equivalent to a trivial braid with both end-nodes in the same state (e.g., Fig. 20). Recall that an actively interacting braid is studied most conveniently in its trivial representation, which should read $S_{T_r}[T_a, T_b, T_c]_{T_r}^S$.

Figure 20: The braid B in 18 is equivalent to a trivial braid.

The discussion above is all about direct right-interaction. **Direct left-interaction** is defined analogously and can be visualized as the left-right mirror image of right-interaction. Thus, in the sequel, we assume direct left-interaction is understood. We denote a direct interaction of two braids B_1 and B_2 by $B_1 +_d B_2 = B$; whether it is a left- or right-interaction is manifest contextually.

A formal division of braids is now natural. We temporarily denote the set of stable braids by \mathfrak{B}_0^S . Nevertheless, for reasons to become transparent we enlarge \mathfrak{B}_0^S by adding two more braids:

$$B_0^\pm = {}_0^\pm[0, 0, 0]_0^\pm, \quad (3.5)$$

which are completely trivial¹⁴. B_0^\pm are actually unstable because they are dual to a 3-ball. If we tolerate their instability they are obviously actively interacting. As such, let us still call the enlarged set the set of stable braids but denote it by \mathfrak{B}^S . \mathfrak{B}^S admits a disjoint union of three subsets:

$$\mathfrak{B}^S = \mathfrak{B}^b \sqcup \mathfrak{B}^f \sqcup \mathfrak{B}^s, \quad (3.6)$$

where \mathfrak{B}^b , \mathfrak{B}^f , and \mathfrak{B}^s are the sets respectively of actively interacting braids (including B_0^\pm), all actively propagating braids that do not actively interact, and stationary braids. Meaning of the superscripts will be clear later. Although actively interacting braids are also actively propagating[6, 10], they are excluded from \mathfrak{B}^f . It is a theorem that $\forall B \in \mathfrak{B}^b$, the effective state of B , $\chi_B \equiv 1$ [8].

We now dwell on the algebra of direct interactions. For simplicity, let us consider $B, B' \in \mathfrak{B}^b$, $B = S_{T_r}[T_a, T_b, T_c]_{T_r}^S$ on the left of $B' = S_{T_r}'[T_a', T_b', T_c']_{T_r}'^S$. If B and B' satisfy the interaction Condition 3.1(1)

¹⁴Note again that at this point spin network labels are not in play. Including spin network labels has two immediate consequences. Firstly, like any other braid in \mathfrak{B}^S , B_0^\pm are not just two braids but infinite ones coloured by different sets of spin network labels. Secondly, B_0^\pm are only trivial topologically but neither algebraically nor physically.

trivially, i.e., if $T_r + T'_l = 0$ and $S = S'$, then the direction interaction of B and B' is simply

$$B +_d B' \stackrel{T_r+T'_l=0}{=} \int_{T_l}^S [(T_a, T_b, T_c) + (T'_a, T'_b, T'_c)]_{T_r}^S = \int_{T_l}^S [T_a + T'_a, T_b + T'_b, T_c + T'_c]_{T_r}^S. \quad (3.7)$$

If, however, B and B' satisfy the interaction condition nontrivially, i.e. if either B 's right end-node or B' 's left end-node must be rotated to make them meet Condition 3.1(1), some algebra is needed. We would refer to [7, 8] for the details; rather, we present the Lemma 3.1 as the general result. Note that we put an actively interacting braid in its trivial representation and an arbitrary braid in its unique representation.

Lemma 3.1. *Given a braid $B = \int_{T_l}^S [T_a, T_b, T_c]_{T_r}^S \in \mathfrak{B}^b$ on the left of a non-actively interacting braid, $B' = \int_0^S [(T'_a, T'_b, T'_c)\sigma_X]_0^{S_r}$, with the interaction condition satisfied by $(-)^{T_r} S = S_l$, the direct interaction of B and B' results in a braid*

$$B'' = \int_0^{(-)^{T_l} S} [((P_{-T_l}^S(T_a, T_b, T_c)) + (P_{-T_l-T_r}^{(-)^{T_r} S}(T'_a, T'_b, T'_c)) + (T_l + T_r, \cdot, \cdot))\sigma_{X_l((-)^{T_r} S, -T_l-T_r)X}]_0^{S_r},$$

where $(T_l + T_r, \cdot, \cdot)$ is the short for $(T_l + T_r, T_l + T_r, T_l + T_r)$.

The P_m^S in the B'' in Lemma 3.1 is a permutation on the triple, determined by S_l and m and valued in the group S_3 . Fig. 14 and its mirror images readily shows $P_{+1}^+ = (1\ 2)$, $P_{-1}^+ = (2\ 3)$, $P_{+1}^- = (3\ 2)$, and $P_{-1}^- = (1\ 2)$. More general equalities can be derived recursively and found in [7]. The functions $X_l(S_l, m)$ and $X_r(S_r, n)$ return crossing sequences generated by the rotations needed to set B 's right end-node and B' 's left end-node ready for a $2 \rightarrow 3$ move. [8] offers their definitions and properties. We show only an example here: $X_l(+, 2k) = (ud)^{-k}$ and $X_l(+, 2k-1) = d(ud)^{-k}$, where $k \in \mathbb{Z}$. A positive exponent of a crossing sequence means, for example, $(ud)^2 = udud$, while a negative one means, for instance, $(ud)^{-2} = d^{-1}u^{-1}d^{-1}u^{-1}$. Lemma 3.1 is independent of the trivial representation chosen for B [8]. Eq. 3.7 is merely a special case of Lemma 3.1. We are now ready for a main result.

Theorem 3.1. *Given $B = \int_{T_l}^S [T_a, T_b, T_c]_{T_r}^S \in \mathfrak{B}^b$, and any braid, $B' = \int_0^S [(T'_a, T'_b, T'_c)\sigma_X]_0^{S_r} \in \mathfrak{B}^S$, such that $B + B' = B'' \in \mathfrak{B}^S$, the effective twist number Θ is an additive conserved quantity, while the effective state χ is a multiplicative conserved quantity, namely*

$$\begin{aligned} \Theta_{B''} &= \Theta_B + \Theta_{B'} \\ \chi_{B''} &= \chi_B \chi_{B'}. \end{aligned} \quad (3.8)$$

This theorem, proved in [8], demonstrates that the two invariants of equivalence moves of braids, Θ and χ , are also conserved charges of direct interactions. Conservation laws play a pivotal role in revealing the underlying structure of a physical theory. By invariants and conserved quantities we are able to determine how the content of our theory may relate to particle physics and if extra inputs are compulsory. In Section 3.6, we try to identify our conserved quantities with particle quantum numbers.

Since $\chi_B \equiv 1 \forall B \in \mathfrak{B}^b$, Theorem 3.1 shows that if B directly interact with a braid with $\chi = -1$, the result must be a braid with $\chi = -1$ too and is thus not in \mathfrak{B}^b . Moreover, $\mathfrak{B}^b +_d \mathfrak{B}^S \setminus \mathfrak{B}^b \subseteq \mathfrak{B}^S \setminus \mathfrak{B}^b$.

Because fermions usually do not directly interact with each other but can interact with (gauge) bosons, that a direct interaction always involve at least one actively interacting braid implies an analogy between actively (non-actively) interacting braids and bosons (fermions). The evidence of this analogy will become stronger soon, after we study exchange interaction. This analogy manifests the meaning of the superscript “ b ”, as for bosons, of \mathfrak{B}^b , the set of actively interacting braids. As to the set of non-actively interacting braids, we divided it into \mathfrak{B}^f and \mathfrak{B}^s , and we are more inclined to consider the former analogous to the set of fermions because the braids in \mathfrak{B}^f are chiral[6], analogous to that the SM elementary fermions are chiral, which manifest the superscript “ f ” in \mathfrak{B}^f .

The result of a direct interaction of two braids is unique! Nonetheless, this uniqueness may cease to hold if the braided ribbon networks are graced with spin network labels, such that the result of an evolution move becomes a superposition of outcomes with the same topology but different sets of labels.

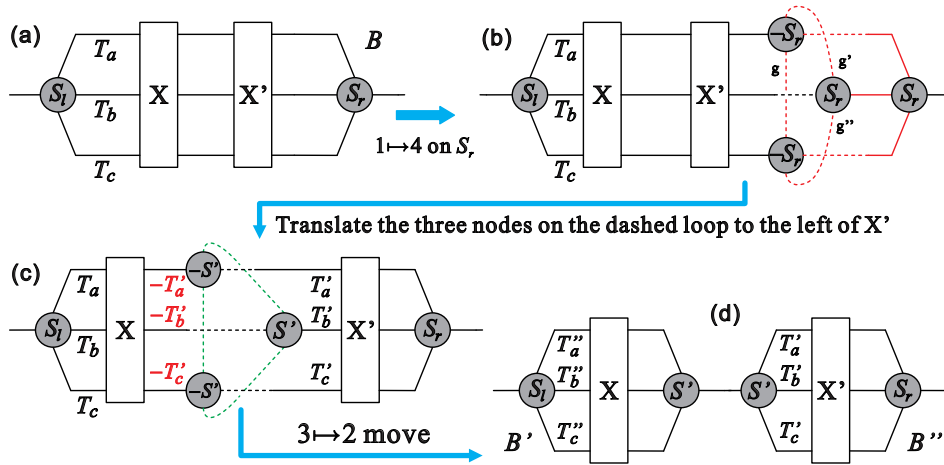


Figure 21: Definition of braid decay: $B \xrightarrow{\rightsquigarrow} B' + B''$, $B, B' \in \mathfrak{B}^S$, $B'' \in \mathfrak{B}^b$. The dashed lines emphasize the dependence of their relative positions on the state S_r .

It is natural to ask if a braid can decay, like a particle. The answer is Yes. A braid decay is a reversed process of a direct interaction. Hence, through decay a braid always radiates an actively interacting braid, on its left or its right. We thus differentiate a left-decay from a right-decay, which are symbolized respectively by $B \xrightarrow{\rightsquigarrow} B' + B''$, indicating that $B' \in \mathfrak{B}^b$, and $B \xrightarrow{\rightsquigarrow} B' + B''$ because $B'' \in \mathfrak{B}^b$.

Fig. 21 defines right-decay. Fig. 21(a) shows a right-reducible braid, $B = {}^S[(T_a, T_b, T_c)\sigma_{XX'}]^{S_r}$, with a chosen reducible crossing segment X' , $X' \leq X_{maxred} \leq X$, where X_{maxred} is the maximal reducible segment of X . This indicates that, in contrast to direct interaction, a braid may decay in multiple ways, each corresponding to a choice X' that must be specified in a decay process. As the reverse of direct left-interaction, Fig. 21 should be easily understood, whose algebraic form is

$$B = {}^S[(T_a, T_b, T_c)\sigma_{XX'}]^{S_r} \xrightarrow{\rightsquigarrow} {}^S[(T_a, T_b, T_c) - \sigma_X^{-1}(T'_a, T'_b, T'_c)]\sigma_X]^{S'} + {}^S[(T'_a, T'_b, T'_c)\sigma_{X'}]^{S_r} = B' + B'', \quad (3.9)$$

where $S' = (-)^{|X'|}S_r$, $B'' \in \mathfrak{B}^b$, and the “+” denotes the adjacency of B' and B'' . Left-decay is defined similarly. The relation between decay and direct interaction ensures that effective twist Θ and effective state χ are also additively and multiplicatively conserved in braid decay.

Not only a reducible braid but also an irreducible - in fact any - braid can radiate. What an irreducible braid emits is but either of B_0^\pm in Eq. 3.5. In fact, because a $1 \rightarrow 4$ can always take place on either end-node of any braid, a subsequent $3 \rightarrow 2$ on three of the four nodes generated by the $1 \rightarrow 4$ move results in either a B_0^+ or a B_0^- , depending on the state of the end-node. This is why B_0^\pm are included in \mathfrak{B}^S although they are unstable. It is therefore plausible that B_0^\pm are analogous to gravitons.

We now proceed to the exchange interaction of braids. Unlike a direct interaction, an exchange interaction can be defined on the whole \mathfrak{B}^S as a map, $+_e : \mathfrak{B}^S \times \mathfrak{B}^S \rightarrow \mathfrak{B}^S \times \mathfrak{B}^S$. Exchange interaction gets its name because each such process always involves an exchange of a virtual actively interacting braid. It is useful to keep track of the direction of the flow of the actively interacting braid during an exchange interaction. Therefore, we differentiate a *left* and a *right exchange interaction*, respectively denoted by $\overleftarrow{+}_e$ and $\overrightarrow{+}_e$. The arrow indicates the “flow” of the virtual actively interacting braid.

The graphic definition of **right exchange interaction** is illustrated in Fig. 22. The left exchange interaction is defined likewise. We now make a few remarks.

Firstly, we begin with the $B_1 = {}^S[(T_{1a}, T_{1b}, T_{1c})\sigma_{X_{1A}X_{1B}}]^{S_r}$ and $B_2 = {}^S[(T_{2a}, T_{2b}, T_{2c})\sigma_{X_2}]^{S_{2r}}$, which are two stable braids, in Fig. 22(a). The zero external twists are omitted as B_1 and B_2 are in their unique representations. B_1 's right end-node and B_2 's left end-node are set in the same state, S , to satisfy the interaction condition. We also assume that B_1 has a reducible crossing segment, say X_{1B} .

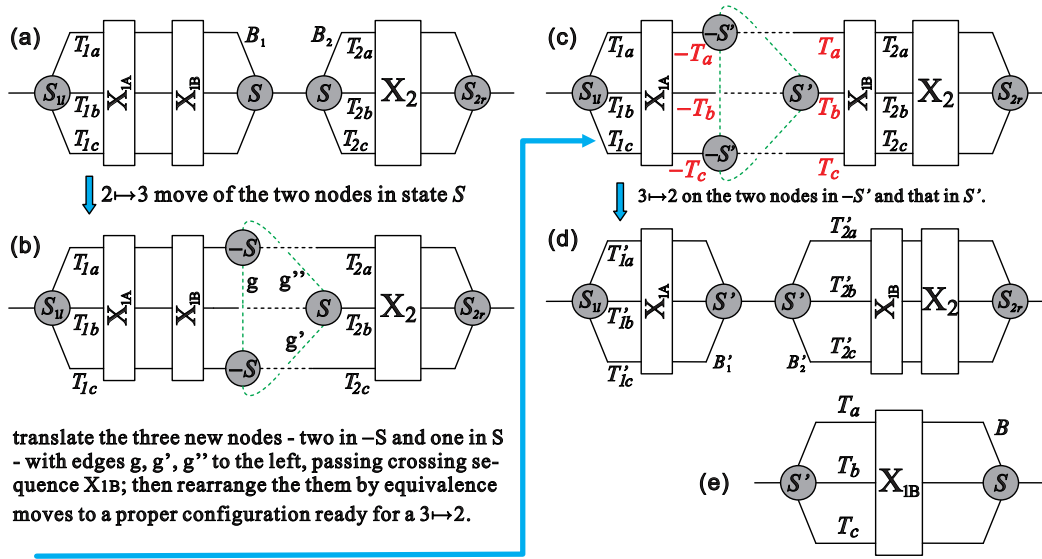


Figure 22: (a)-(d): Definition of right exchange interaction: $B_1 \vec{+}_c B_2 \rightarrow B'_1 + B'_2$, $B_1, B_2, B'_1, B'_2 \in \mathfrak{B}^S$. (e) The virtual actively interacting braid exchanged from B_1 to B_2 .

Secondly, if X_{1B} is not trivial, i.e., if B_1 is right-reducible, translating the three nodes on the loop in (b) and rearranging them by equivalence moves into a proper configuration ready for a 3 \rightarrow 2 move generates a pair of triples of internal twists, $-(T_a, T_b, T_c)$ and (T_a, T_b, T_c) , and causes $S' = (-)^{|X_{1B}|}S$, as in (c). Taking the permutations induced by X_{1A} and by X_{1B} into account, in (d) we have the relations:

$$(T'_{1a}, T'_{1b}, T'_{1c}) = (T_{1a}, T_{1b}, T_{1c}) - \sigma_{X_{1A}}^{-1}(T_a, T_b, T_c) \quad (3.10)$$

$$(T'_{2a}, T'_{2b}, T'_{2c}) = (T_a, T_b, T_c) + \sigma_{X_{1B}}^{-1}(T_{2a}, T_{2b}, T_{2c}), \quad (3.11)$$

which produce the two adjacent braids, B'_1 and B'_2 , related to B_1 and B_2 .

Thirdly, according to direct interaction, the only possible triple (T_a, T_b, T_c) in Fig. 22(c) is exactly the same as the triple of internal twists of an actively interacting braid - $B = {}^S[(T_a, T_b, T_c)\sigma_{X_{1B}}]^S$ - in Fig. 22(e). For an actively interacting braid of the form in Fig. 22(e), $S' = (-)^{|X_{1B}|}S$; hence, B' 's left and right end-nodes are respectively in the same states as that of the left end-node of B'_2 in Fig. 22(d) and that of the right end-node of B_1 in Fig. 22(a). Thus, the form of braid B'_2 in Fig. 22(d) must be precisely the result of the direct interaction of B and B_2 , which by Lemma 3.1 is

$$B +_d B_2 = {}^{S'}[(T_a, T_b, T_c) + \sigma_{X_{1B}}^{-1}(T_{2a}, T_{2b}, T_{2c})\sigma_{X_2}]^{S_{2r}} = B'_2,$$

which validates the relation in Eq. 3.11.

Therefore, the process of the right exchange interaction defined in Fig. 22 is as if B_1 and B_2 interact with each other via exchanging a virtual actively interacting braid B , then become B'_1 and B'_2 . Or one may say that an exchange interaction is mediated by an actively interacting braid. This reinforces the analogy between actively interacting braids and bosons¹⁵. Note that in an exchange interaction, there does not exist an intermediate state in which only the virtual actively interacting braid is present because our definition of a braid requires the presence of its two end-nodes. The following theorem summarizes the above as another main result. (The case of left exchange interaction is similar.)

Theorem 3.2. *Given two adjacent braids, $B_1, B_2 \in \mathfrak{B}^S$. $B_1 = {}^S[(T_{1a}, T_{1b}, T_{1c})\sigma_{X_{1A}X_{1B}}]^S$ is on the left and has a reducible crossing segment X_{1B} , and $B_2 = {}^S[(T_{2a}, T_{2b}, T_{2c})\sigma_{X_2}]^{S_{2r}}$, there exists a braid $B \in \mathfrak{B}^B$,*

¹⁵More generally, this should imply the analogy between actively interacting braids and particles that mediate interactions, which should potentially include super partners of gauge bosons.

$B = S'[(T_a, T_b, T_c)\sigma_{X_{1B}}]^S$ with $S' = (-)^{|X_{1B}|}S$, such that it mediates the exchange interaction of B_1 and B_2 to create $B'_1, B'_2 \in \mathfrak{B}^S$, i.e.,

$$\begin{aligned} B_1 \vec{+}_e B_2 &\rightarrow B'_1 + B'_2 \\ &= S^{1r}[(T_{1a}, T_{1b}, T_{1c}) - \sigma_{X_{1A}}^{-1}(T_a, T_b, T_c)\sigma_{X_{1A}}]^{S'} + S'[(T_a, T_b, T_c) + \sigma_{X_{1B}}^{-1}(T_{2a}, T_{2b}, T_{2c})\sigma_{X_2}]^{S_{2r}}. \end{aligned} \quad (3.12)$$

The fourth remark is, if $X_{1B} = \mathbb{I}$, however, $(T_a, T_b, T_c) = (0, 0, 0)$, and hence $(T'_{1a}, T'_{1b}, T'_{1c}) = (T_{1a}, T_{1b}, T_{1c})$, $(T'_{2a}, T'_{2b}, T'_{2c}) = (T_a, T_b, T_c)$, and $S' = S$. That is, $B'_1 = B_1$ and $B'_2 = B_2$. Thus, the virtual actively interacting braid exchanged in the interaction is either B_0^+ or B_0^- , which were aforementioned to be analogous to gravitons.

Here is the final remark. By the same reason why a braid can decay in multiple ways, two braids can have exchange interactions in more than one ways too, as opposed to direct interaction. This non-uniqueness of exchange interaction has an analogy in particle physics. For instance, quarks have both electric and color charges, both photons and gluons can mediate forces on quarks. The relation between actively interacting braids and bosons is yet not an actual identification, however. In fact, if each actively interacting braid corresponded to a boson, there would be too many "bosons". The underlining physics of that two braids can have exchange interactions in different ways deserves further studies.

It should be emphasized that each individual exchange interaction is a process that yields a unique result¹⁶. An expression like $B_1 \vec{+}_e B_2$ is only formal. Only when the exact forms of B_1 and B_2 with their reducible segments are explicitly given, $B_1 \vec{+}_e B_2$ acquires a precise and unique meaning. In computing an exchange interaction, we have to specify our choice of the reducible crossing segment of the braid that gives out the virtual actively interacting braid. For any such choice Theorem 3.2 holds.

The following Theorem shows that the additive and multiplicative conserved quantities of direct interaction in Theorem 3.1 are also conserved in the same manner under exchange interaction.

Theorem 3.3. *Given two neighbouring stable braids, $B_1, B_2 \in \mathfrak{B}^S$, such that an exchange interaction (left or right or both) on them is doable, i.e., $B_1 +_e B_2 \rightarrow B'_1 + B'_2$, $B'_1, B'_2 \in \mathfrak{B}^S$, the effective twist Θ is an additive conserved quantity, while the effective state χ is a multiplicative conserved quantity, namely*

$$\begin{aligned} \Theta_{B'_1} + \Theta_{B'_2} &\stackrel{+e}{=} \Theta_{B_1} + \Theta_{B_2} \\ \chi_{B'_1} \chi_{B'_2} &\stackrel{+e}{=} \chi_{B_1} \chi_{B_2}, \end{aligned} \quad (3.13)$$

independent of the virtual actively interacting braid being exchanged during the exchange interaction.

This Theorem is proved in [10]. Consequently, exchanges of actively interacting braids give rise to interactions between braids that are charged under the topological conservation rules. The conservation of Θ is analogous to the charge conservation in particle physics.

3.6 Dynamics: CPT and Braid Feynman Diagrams

In this Section we discuss the charge conjugation, parity, and time reversal symmetries of stable braids, and the braid Feynman diagrams. We shall present some key results with a few remarks.

3.6.1 C, P, and T

Though not separately, as a theorem the combined action CPT is a symmetry in any Lorentz invariant, local field theory. Being a physical model of QFT, the SM respects the CPT-symmetry too. This urges the search for the possible discrete, non-equivalence, transformations of 4-valent braids and check their correspondence with C, P, and T transformations. Whether our braids would eventually be mapped to or

¹⁶With spin network labels the result is not unique any more because two topologically equal braids can be decorated by different sets of labels, and an interaction should result in a superposition of braids labelled differently.

more fundamental than the SM particles, they should possess quantum numbers that are transformed by C, P, and T. Conversely, investigating the action of discrete transformations on our braid excitations can help us to construct quantum numbers of a braid.

A large number of possible discrete transformations of the 4-valent braids exist, however, e.g., the permutation group S_3 on the triple of internal twist, several copies of \mathbb{Z}_2 that flip a twist, an end-node state, and a crossing respectively, etc.. The challenge then is to filter out the unwanted discrete transformations. Surprisingly, the braid dynamics introduced above turns out to naturally select exactly seven legal discrete transformations of the braids, as C, P, T, and their products add up to seven in total (eight including identity). Now we show how this ‘‘super-selection’’ works. In view of that QFT does not bear a transformation that magically changes a particle to something else, the dynamics of the braids of embedded 4-valent spin networks, namely propagation and interaction, naturally constrains what discrete transformations are allowed on braids, which is summarized as a guideline in the following Condition.

Condition 3.2. *A legal discrete transformation \mathcal{D} on an arbitrary braid B must be an automorphism on \mathcal{B}^b , \mathcal{B}^f , and \mathcal{B}^s separately.*

We expect the discrete transformations to be representation independent; therefore, the study of their effects should be made on braids in their generic forms (Fig. 13(a) and Eq. 3.1). Table 1 displays the result, in which explicit identification of the legal discrete transformations with C, P, and T is made.

Discrete Transformation	Action on $B = \overset{S_l}{T_l}[(T_a, T_b, T_c)\sigma_X]_{T_r}^{\overset{S_r}{T_r}}$	Prop-Direction	Action on $ \mathbf{p}, \sigma, n\rangle$
$\mathbb{1}$	$\overset{S_l}{T_l}[(T_a, T_b, T_c)\sigma_X]_{T_r}^{\overset{S_r}{T_r}}$	+	$ \mathbf{p}, \sigma, n\rangle$
C	$\overset{\bar{S}_l}{-T_l}[-(T_a, T_b, T_c)\sigma_{I_X(X)}]_{-T_r}^{\bar{S}_r}$	+	$\propto \mathbf{p}, \sigma, n^c\rangle$
\mathcal{P}	$\overset{\bar{S}_r}{T_r}[(T_{a'}, T_{b'}, T_{c'})\sigma_{\mathcal{R}(X)}]_{T_l}^{\bar{S}_l}$	-	$\propto -\mathbf{p}, \sigma, n\rangle$
\mathcal{T}	$\overset{S_r}{T_r}[(T_{c'}, T_{b'}, T_{a'})\sigma_{\mathcal{S}_c\mathcal{R}(X)}]_{T_l}^{\overset{S_l}{T_l}}$	-	$\propto (-)^{J-\sigma} -\mathbf{p}, -\sigma, n\rangle$
$C\mathcal{P}$	$\overset{\bar{S}_r}{-T_r}[-(T_{a'}, T_{b'}, T_{c'})\sigma_{X^{-1}}]_{-T_l}^{\bar{S}_l}$	-	$\propto -\mathbf{p}, \sigma, n^c\rangle$
$C\mathcal{T}$	$\overset{\bar{S}_r}{-T_r}[-(T_{c'}, T_{b'}, T_{a'})\sigma_{I_X\mathcal{S}_c\mathcal{R}(X)}]_{-T_l}^{\bar{S}_l}$	-	$\propto (-)^{J-\sigma} -\mathbf{p}, -\sigma, n^c\rangle$
$\mathcal{P}\mathcal{T}$	$\overset{\bar{S}_l}{T_l}[(T_c, T_b, T_a)\sigma_{\mathcal{S}_c(X)}]_{T_r}^{\bar{S}_r}$	+	$\propto (-)^{J-\sigma} \mathbf{p}, -\sigma, n\rangle$
$C\mathcal{P}\mathcal{T}$	$\overset{\bar{S}_l}{-T_l}[-(T_c, T_b, T_a)\sigma_{I_X\mathcal{S}_c(X)}]_{-T_r}^{\bar{S}_r}$	+	$\propto (-)^{J-\sigma} \mathbf{p}, -\sigma, n^c\rangle$

Table 1: The group of discrete transformations on a generic braid diagram. In column-3, a - (+) means the propagation direction of the braid is flipped (unaffected). For comparison, column-4 is the action of the group on a one-particle state, with 3-momentum \mathbf{p} , 3rd component σ of spin J , and charge n .

In column-2 of Table 1, \mathcal{R} , I_X , and \mathcal{S}_c are discrete operations on the crossing sequence X of a braid, respectively defined by $\mathcal{R} : X = x_1 x_2 \cdots x_n \mapsto x_n x_{n-1} \cdots x_1$, $I_X : X = x_1 x_2 \cdots x_n \mapsto x_1^{-1} x_2^{-1} \cdots x_n^{-1}$, and $\mathcal{S}_c : \forall x_i \in X, x_i \mapsto d$ if $x_i = u$ and $x_i \mapsto u$ if $x_i = d$. Hence, $X^{-1} = I_X \mathcal{R}(X)$. Note that $\sigma_X^{-1} \neq \sigma_{X^{-1}}$ in general. These operations are commutative and are elaborated in [9, 17].

In Table 1, we chose to denote C, P, and T transformations in the Hilbert space by calligraphic letters C , \mathcal{P} , and \mathcal{T} because braids are topological excitations of embedded spin networks that are the states in the Hilbert space describing the fundamental spacetime. One can easily check that the eight discrete transformations including identity in the first column of Table 1 indeed form a group, which is actually

the largest group of legal discrete transformations of 3-strand braids[9, 17]. This is the first reason why they can be identified with C, P, T, and their products.

We emphasize again that these discrete transformations of braids are not equivalence moves; they take a braid to inequivalent ones, as seen in Table 1. Staring at the 3rd column of the table, one readily finds that some characterizing quantities of a braid, e.g., the effective twist and effective state, are invariant under some transformations but not under others. Table 1 is obtained by utilizing these topological characterizing quantities, without involving spin network labels. We do not count in the phase and sign factors in the 4th column of Table 1 either. All the transformations are restricted to local braid states, rather than a full evolution picture. Given these, surprisingly, the map between the legal discrete transformations of braids and those on single particle states appears to be unique.

According to column-4 in Table 1, the transformations \mathcal{P} , \mathcal{T} , $C\mathcal{P}$, and $C\mathcal{T}$ reverse the three momentum of a one-particle state. But then, what is the momentum of a braid? Fortunately, we need not to explicitly define the 3-momentum of a braid for the moment to tell the discrete transformations that can flip the momentum because it should always agrees with the braid's local propagation direction, however it is defined[9]. Therefore, the discrete transformations reversing the 3-momentum of a braid are exactly those flipping the propagation direction of the braid. This also helps to pins down Table 1.

The effective twist Θ and effective state χ are representation-independent invariants and dynamically conserved quantities of a braid, while charges, e.g., electric and color charges, are quantum numbers of a particle. Hence, only Θ , χ , and functions of them can be candidates for certain charges of a braid. As we know, the electric charge of a particle is an integral multiple of $1/3$, an additively conserved quantity, and a result of $U(1)$ gauge symmetry. The effective twist of a braid has three similar traits. We have seen the first two and now talk about the third property. The framing that inflate a spin network edge to a tube is in fact a $U(1)$ framing. That is, a tube is essentially an isomorphism from $U(1)$ to $U(1)$, which is characterized by its twists. A twist-free tube is an identity map, whereas a twisted tube represents a non-trivial isomorphism. These suggest to interpret Θ or an appropriate function of it as the "electric charge" of a braid, which may in turn explains the origin and quantization of electric charge.

Here is the final remark on Table 1. On a single particle state, a $C\mathcal{P}\mathcal{T}$ has one more effect than a C because it also turns σ , the z -component spin, to $-\sigma$. Although we do not know yet what of a braid corresponds to σ , we can still nail down the $C\mathcal{P}\mathcal{T}$. [9, 17] argue that spin network labels should play the role that determines the "spin" of a braid state.

The C, P, and T group stable braids into CPT-multiplets. The braids in a multiplet are not equivalent but may share some traits. It would be heuristic to find how a CPT-multiplet of braids is characterized. Theorem 3.4 shows that only CPT-multiplets of actively interacting braids have a topological character.

Theorem 3.4. *All actively interacting braids in a CPT-multiplet have the same number of crossings if each of them is in its unique representation. This number uniquely characterizes the CPT-multiplet.*

The proof of the theorem can be found in [9, 17]. Theorem 3.4 does not apply to non-actively interacting braids. In fact, we can always find two non-actively interacting braids with m crossings ($m > 1$), in their unique representations, which are not related to each other by any discrete transformation. For example, the 2-crossing braids $S[(T_a, T_b, T_c)\sigma_{ud-1}]^{S_r}$ and $S'[(T'_a, T'_b, T'_c)\sigma_{uu}]^{S'_r}$ can never belong to the same CPT-multiplet, regardless of their internal twists and end-node states. Nevertheless, it is still true that *all the non-actively interacting braids in a CPT-multiplet have the same number of crossings if they are in the same type of representation*[9]. This is simply because the discrete transformations do not alter the representation type and the number of crossings of a braid.

Having seen the effects of C, P, and T on single braid excitations, we now discuss the action of these discrete transformations on braid interactions. *Braid interactions turn out to be invariant under CPT, and more precisely, under C, P, and T separately*[9, 10]. By this we mean, say, for a direct interaction under a C, $C(B) +_d C(B') = C(B +_d B')$, while under a P, it means $\mathcal{P}(B') +_d \mathcal{P}(B) = \mathcal{P}(B +_d B')$. Note that the P-transformation of a direct interaction swaps its direction. A subtlety arises in the case of T, however. An interaction involves the time evolution of a spin network. To apply our T-transformation to an interaction,

one should reverse all the dynamical moves. Hence, a T-transformation turns a direct interaction into a decay. That is, to show the invariance of $B +_d B' \rightarrow B''$ under time reversal, it suffices to show that $\mathcal{T}(B'') \xrightarrow{\sim} \mathcal{T}(B') + \mathcal{T}(B)$. Analogous, the invariance of an exchange interaction, $B_1 \vec{+}_e B_2 \rightarrow B'_1 + B'_2$, under time reversal reads $\mathcal{T}(B'_2) \vec{+}_e \mathcal{T}(B'_1) \rightarrow \mathcal{T}(B_2) + \mathcal{T}(B_1)$. The case of braid decay follows similarly[10].

This observation of the absence of CP-violation in our theory does not comply with the SM of particles, which seems to infer an issue that the interactions of braids are deterministic, in the sense that an interaction of two braids produces a definite new braid. Nevertheless, this may not be a problem at all because we have only worked with definite vertices of interactions. In terms of vertices we have definite result for an interaction as to the case in QFT; this is similar to what have been done in SF models or GFTs. Besides, one can certainly argue that if our braids are more fundamental entities, the CP-violation in particle physics need not to hold at this level. Putting this CP-violation problem aside, however, a fully quantum mechanical picture should be probabilistic¹⁷.

If the absence of CP-violation was truly an issue, we would consider braids with the same topological structure but different sets of spin network labels as physically different. One may adapt some SF methods to assign amplitudes to the adapted dual Pachner moves of the braided ribbon networks. An evolution move may then yield outcomes with the same topological configuration but different spin network labels; each outcome has a certain probability amplitude. As a result, an interaction of two braids may give rise to superposed braids, each of which has a certain probability to be observed, with the same topological content but different set of spin network labels. With this, CP-violating interactions may arise.

Note that the current study of discrete transformations of braids would not be impact by just adding spin network labels in a straightforward way in to our scheme. A reason is that the discrete transformations of the braids do not change the spin network label of each existing edge of the network. One may try to construct discrete transformation that change the spin network labels on braids, but one does not have *a priori* a reason to make a special choice among many arbitrary ways of doing this.

3.6.2 Asymmetry of Braid Interaction

Both direct and exchange interactions are asymmetric. A brief description is as follows. That direct interaction is asymmetric means: Given an actively interacting braid B and an arbitrary braid B' , in general either of the direct right interaction $B +_d B'$ or the left interaction $B' +_d B$ cannot occur because of the violation of the corresponding interaction condition. Even if both interactions are feasible, $B +_d B'$ and $B' +_d B$ are two inequivalent braids in general, which reads $B +_d B' \not\cong B' +_d B$. Two exceptions exist. In the cases where B and B' meet certain constraints, $B +_d B'$ and $B' +_d B$ can simply be equal[8].

On the other hand, interestingly, $B +_d B'$ and $B' +_d B$ can be related by discrete transformations. Because P-transformation swaps the two braids undergoing a direct interaction, i.e., $\mathcal{P}(B +_d B') = \mathcal{P}(B') +_d \mathcal{P}(B)$, we immediately have

$$B' +_d B = \mathcal{P}(B +_d B'), \text{ if } B = \mathcal{P}(B), B' = \mathcal{P}(B') \quad (3.14)$$

where the \mathcal{P} can be replaced by $C\mathcal{P}$ by the same token. Note that, however, time reversal cannot relate $B +_d B'$ and $B' +_d B$ because it turns a direct interaction into a decay.

As aforementioned, the set of actively interacting braids is closed under direct interaction. This and the asymmetry of direct interaction then give rise to the following theorem[6, 8].

Theorem 3.5. *The set of actively interacting braids \mathfrak{B}^b is an algebra under direct interaction, namely $\mathfrak{B}^b +_d \mathfrak{B}^b = \mathfrak{B}^b$. This algebra is associative and non-commutative.*

It follows that braid decay also asymmetric but we shall skip this and move on to the asymmetry of exchange interaction, which is subtler.

The asymmetry of exchange interaction is three-fold. Firstly, for $B_1, B_2 \in \mathfrak{B}^s$, in general $B_1 \vec{+}_e B_2 \not\cong B_2 \vec{+}_e B_1$ ($B_1 \vec{+}_e B_2 \not\cong B_2 \vec{+}_e B_1$), which is called the **asymmetry of the first kind**. Secondly, in general

¹⁷One should note that a few theoretical physicists may not agree on this.

$B_1 \vec{\mp}_e B_2 \neq B_1 \overleftarrow{\mp}_e B_2$, which is christened the **asymmetry of the second kind**. The **asymmetry of the third kind** states that generically $B_1 \vec{\mp}_e B_2 \neq B_2 \vec{\mp}_e B_1$. As in the case of direct interaction, when B_1 and B_2 satisfy certain constraints, symmetric exchange interactions arise; however, a subtlety should be noted. Since two braids may have different exchange interactions, $B_1 \vec{\mp}_e B_2$ and $B_2 \vec{\mp}_e B_1$ cannot be equal for all possible ways of how B_1 and B_2 may interact. The right question to ask is, taking right exchange interaction as an example: For any B_1 and B_2 , do there exist an instance of $B_1 \vec{\mp}_e B_2$ and one of $B_2 \vec{\mp}_e B_1$ among all possible ways of these two interactions, such that $B_1 \vec{\mp}_e B_2 = B_2 \vec{\mp}_e B_1$? [10] answers this question for the first two kinds of asymmetry. This asymmetry of the third kind is new and not studied in [10] but it would not be hard by following the derivations in [10].

Like direct interactions, asymmetric exchange interactions may be related by discrete transformations, but only for the asymmetry of the third kind. Since in the asymmetry of the third kind, the positions of the braids and the interaction direction are both swapped, we immediately see that only P and CP are able to do this. Therefore, we obtain Eq. 3.15, in which \mathcal{P} can be replaced by $C\mathcal{P}$.

$$B_2 \overleftarrow{\mp}_e B_1 = \mathcal{P}(B_1 \vec{\mp}_e B_2), \text{ if } B_1 = \mathcal{P}(B_1), B_2 = \mathcal{P}(B_2). \quad (3.15)$$

3.6.3 Braid Feynman Diagrams

An effective theory of the dynamics of 4-valent braids based on Feynman diagrams is possible, which are called **braid Feynman diagrams**. Unlike the usual QFT Feynman diagrams having no internal structure, each braid Feynman diagram is an effective description of the whole dynamical process of a braid interaction and has internal structures that record the evolution of the braid and its ambient.

We use $\bullet \rightarrow$ and $\rightarrow \bullet$ for respectively outgoing and ingoing braids in \mathfrak{B}^f , $\bullet \dashrightarrow$ and $\dashrightarrow \bullet$ for respectively outgoing and ingoing non-actively propagating braids¹⁸ in \mathfrak{B}^s . Outgoing and ingoing braids in \mathfrak{B}^b are better represented by $\bullet \rightsquigarrow$ and $\rightsquigarrow \bullet$ respectively.

In accordance with left and right-decay, we will henceforth denote left and right direct interactions by $\overleftarrow{\mp}_d$ and $\overrightarrow{\mp}_d$ respectively. Note that if the two braids being interacting are both in \mathfrak{B}^b , the direction of the direct interaction is irrelevant because the result is independent of which of the two braids plays the active role in the interaction. Since $\mathfrak{B}^b \overrightarrow{\mp}_d \mathfrak{B}^b \subseteq \mathfrak{B}^b$ and $\mathfrak{B}^b \overrightarrow{\mp}_d (\mathfrak{B}^f \sqcup \mathfrak{B}^s) \subseteq \mathfrak{B}^f \sqcup \mathfrak{B}^s$, the only possible single vertices of right direct interaction and of right decay are respectively listed in Fig. 23(a) and (b), whose left-right mirror images are vertices of direct left-interaction and left-decay. The arrows over the

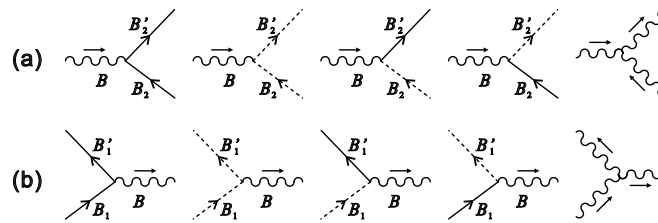


Figure 23: (a) All vertices of direct right-interaction. (b) All vertices of right-decay. Time flows up.

wavy lines in Fig. 23 are important for they differentiate a direct interaction from a decay.

Fig. 24 depicts all possible basic 2-vertex diagrams for right exchange interaction, whose left-right mirror images are certainly the basic diagrams for left exchange interaction. These diagrams manifests the invariance of the exchange interaction under the C, P, T and their products.

Whether an exchange interaction can have symmetric instances is lucid in its diagram. Taking the asymmetry of the first kind as an example, if a diagram looks formally the same as its left-right mirror image with the arrow over the virtual braid not mirrored, the corresponding exchange interaction allows symmetric instances. It follows that Fig. 24(a), (b), (e), (f), (p), and (u)-(x) are such diagrams.

¹⁸These braids can still propagate in an induced way.

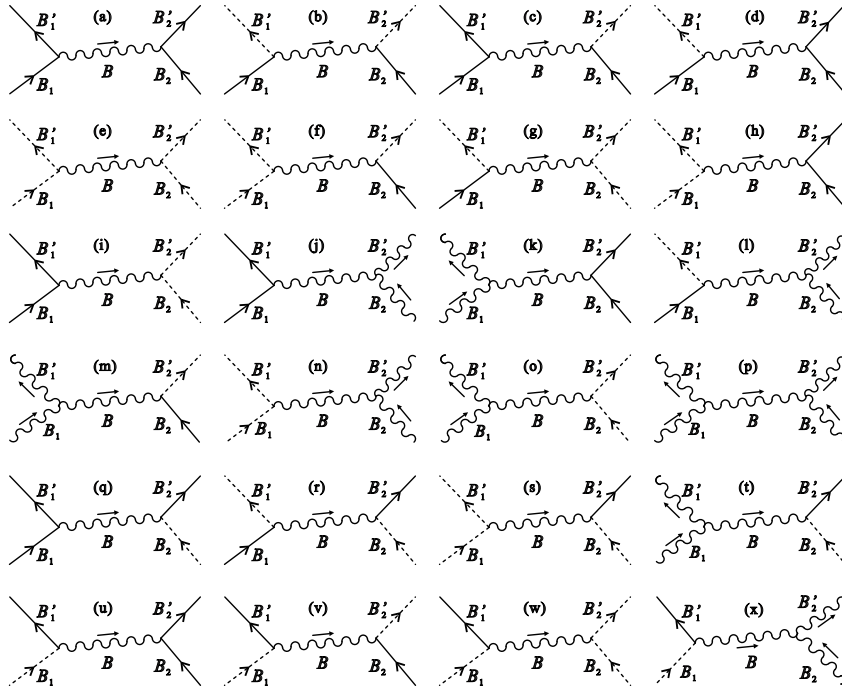


Figure 24: Possible right exchange interaction 2-vertices. Time flows up.

The diagrams in Figures. 23 and 24 crystallizes the analogy between braids in \mathfrak{B}^b and bosons, as the topological conservation laws permit them to be singly created and destroyed and as exchanges of these excitations give rise to interactions between braids charged under the topological conservation rules.

Multi-vertex and loop braid Feynman diagrams can be constructed out of these basic vertices. As a result, there should exist an effective field theory based on these diagrams, in which the probability amplitudes of each diagram can be computed. For this one should figure out the terms evaluating external lines, vertices, and propagators of braids. In a more complete sense, an action of the effective fields representing braids that can generate these braid Feynman diagrams should be devised. Each effective field is a function of the representations of the group elements in the characterizing 8-tuple (and spin network labels if necessary) of a braid; these representations label a line in the corresponding braid Feynman diagram. An easier task is to assign a reasonable probability amplitude of each braid Feynman diagram. In either case, the very first challenge is to find an appropriate mathematical language to study the 4-valent scheme analytically. In the next section we will briefly mention three possible formalisms.

3.7 Discussions and Outlook

The 4-valent scheme resolves some issues and limitations persisting in the 3-valent approach but also raises new issues. In the first place, we obtain a $(3 + 1)$ -dimensional evolution of quantum states of spacetime, which has intrinsic dynamics of the braid excitations of these states. Because of the framing and embedding of spin networks, strands of a braid excitation admit twists only in units of $1/3$. The twists of a braid is directly related to its electric charge, which naturally, rather than by hand, gives rise to charge quantization and fractional charges such as quark charges. The 4-valent theory also contains another natural selection: braid dynamics magically picks out a group of exactly eight discrete transformation, including identity, which can be identified with analogues of C , P , T , and their products.

Some issues the 4-valent scheme raises have been discussed more or less previously. In the sequel, we shall analyse some issues that bear on the interpretation of these results. In the last section, however, we shall introduce ideas, future work, and work in progress, which may remove these issues.

Stability and locality

We argued that the stable braids are local excitations of 4-valent braided ribbon networks because they are noiseless subsystems of the networks. Nevertheless, the comparison with topological field theories that do not bear any local degrees of freedom seems to set the locality of 4-valent braids in doubt. In fact, locality in background independent theories of quantum gravity is delicate, as it is correlated with two other important issues, namely the problem of the concept of spacetime and that of low energy limit. Moreover, the locality and stability of a braid are also entangled.

A background independent quantum gravity theory usually lacks a metric that directly measures spatial locality. But the graph metric of a spin network may define the network locality. In this sense, a stable braid is local because it is confined between two nodes. Unfortunately, the issue in the stability of a braid may damage its locality because Condition 3.1 only protects the a stable braid from being undone but does not prevent the braid's end-nodes from being expanded by $1 \rightarrow 4$ moves. In the latter scenario, the three strands of a braid may turn out to be attached to nodes far from each other on the network, causing the braid nonlocal. We might strengthen the stability condition by further forbidding the action of a $1 \rightarrow 4$ move on either end-node of a stable braid but the pay is the loss of braid decay.

Moreover, the locality discussed above is micro-locality, opposed to which is macro-locality that is defined in the low energy end of the theory. Markopoulou and Smolin proposed these two notions of locality and found that they do not match in general[24], which is also exemplified in [83]. The quantum spacetime in our context is pre-geometric, as it is a sum over quantum histories of superposed pre-geometric spin networks; it is conjectured that continuous spacetime emerge as certain limit of this quantum spacetime. Hence, requiring the micro-locality defined on each spin network to match the macro-locality in continuous spacetime makes no sense.

Macro-locality is more relevant to the known physics; however, it is obtained from micro-locality. This leads back to the problem of low energy limit, to resolve which Markopoulou *et al.* adapted the idea of noiseless subsystems with micro-symmetries from Quantum Information. Therefore, we expect that the symmetry of the braid excitations will induce emergent symmetries, including time and space translation invariance, in the low energy effective description of the braids.

Particle identification and mass

The ultimate physical content of the 4-valent scheme is not fully comprehensible at this stage. In the trivalent scheme, [4] tentatively maps the trivalent braids to SM particles. Whether such a map exists in the 4-valent scheme is yet obscure. A reason is that although the dynamics of 4-valent braids strongly constrains the defining 8-tuple of a stable braid, in particular the actively interacting braids, the closed form of this constraint is still missing. Consequently, we lack for a censorship to pick out the 4-valent braids that may be mapped to SM particles. Nonetheless, we are inclined to another prospect: Braid excitations are fundamental matter whose low energy effective theory yield the SM particles.

If the latter is true, the potential instability and non-locality of stable braids may not be an issue because only the low energy effective counterparts of the braids are physically relevant.

In any case, is how mass arises? Two likelihoods are in order. First, a braid may acquire zero or nonzero mass from some of its intrinsic attributes. Second, mass is not well-defined at the level of spin networks but is emergent in the low energy limit, directly or via certain symmetry breaking. The latter requires working out the effective theory, which is our future work. As to the former, a braid's the number of crossings can be a candidate for its mass (this is also conjectured in the trivalent scheme[2, 4]). Here is the logic. The number of crossings of an actively interacting braid in its unique representation uniquely characterizes the CPT-multiplet the braid belongs to; hence, this number cannot be the charge (already mapped to the braid's effective twists) or 3-momentum of the braid but probably related to the energy of the braid. Besides, actively interacting braids are equivalent to trivial braids, whereas non-actively interacting ones are not. If we associate a braid's mass to its number of crossings, all actively

interacting braids seem massless, consistent with their analogue with (gauge) bosons. and most non-actively interacting braids are massive because they not fully reducible.

Other questions pending for answers

- At the level of spin networks, is there a quantum statistics of braids that can turn the analogy between actively interacting braids and bosons affirmative? If true, are there anyonic braid states?
- Both trivalent and 4-valent schemes need a mechanism to create nontrivial braids on unbraided networks¹⁹. Section 3.7.1 discusses a possible way out.
- Our ansatz that spacetime is fundamentally discrete is partly inspired by the LQG area and volume operators with discrete spectra. Nevertheless, whether these area and volume operators are physical is still under debate[84, 85]. On the one hand, these operators are not gauge invariant. On the other hand, the areas and volumes that we routinely measure are associated to spatial regions determined by matter[86, 64] but LQG was devised to be a theory of gravity only. Now that our program of emergent matter shows that matter may be encoded in LQG as emergent braid excitations of spin networks, it may help to settle the debate.
- Our program of emergent matter is also related to Quantum Graphity, a class of general theories of background independent quantum gravity based on graphs[89, 90]. [87] finds the speed of light²⁰ as a Lieb-Robinson bound[88] in certain Quantum Graphity models. As both trivalent and 4-valent braids can propagate, does a Lieb-Robinson bound of braid propagation exist? The 4-valent scheme expects that actively interacting braids saturate the Lieb-Robinson bound of the system but non-actively interacting ones do not, such that they are respectively massless and massive.

3.7.1 Future directions

We now sketch our plan of reformulating the 4-valent scheme or even our whole program of emergent matter in other frameworks of mathematical physics, such as GFT, Tensor Category, and so on.

Group Field Theories with braids

GFTs²¹ consider d -dimensional simplices the fundamental building blocks of $(d+1)$ -dimensional spacetime and treat them as fields whose variables are elements in the group defining the simplices. That is, a GFT is a local, covariant quantum field theory of universes” in terms of the fields associated with the fundamental building blocks. It would produce a transition amplitude between quantum ”universes” by summing over the Feynman diagrams of this transition, i.e., summing over all triangulations and topologies as the histories built from the evolution of the fundamental d -simplices. These Feynman diagrams can also be viewed as spin networks and dual to $(d+1)$ -simplices. Group Field Theories encompass most of the other approaches to non-perturbative quantum gravity, such as Loop Quantum Gravity and Spin Foam models, provide a link between them, and go beyond the limitations of them[94].

We name two viable routes of formulating a GFT of 4-valent braids. Spin networks are purely combinatoric and unembedded in GFTs, so the first strategy is to enlarge the configuration space of certain $(3+1)$ GFT by adding to its fundamental field group variables that characterize a 4-valent braid.

Inspired by constructing theories of collective modes in condensed matter physics, our second, simpler strategy is to devise a braid field as a composite field of a pair of fundamental group fields whose group variables are identified in a braided way, and then integrate out the fundamental fields to obtain an effective theory of the composite fields in certain background given by the fundamental ones.

¹⁹Trivial braids B_0^\pm in Eq. 3.5 can be otherwise created and annihilated, in the 4-valent scheme.

²⁰This is understood as the maximum speed, at which information can propagate in a system.

²¹The first GFT - the Boulatov model - originated as a generalization of the Matrix Models of 2D gravity to 3D[91]. GFTs in 3D and 4D were realised to be generating theories of Spin Foam models[92, 93]. Later, GFTs are suggested to be fundamental formulations of quantum gravity[94]. [95] presents an extensive review on the subject.

Both ways combine spin network labels automatically and is expected to result in a low energy effective theory of braid excitations in a background spacetime. The former sounds more fundamental and should be able to solve the issue that nontrivial braids cannot be created from spin networks initially free of braids. The latter is what we are currently taking, by which we found it is likely to construct a toy GFT with only certain trivial braids, whose effective theory is a scalar ϕ^4 theory.

Tensor Categorical methods

Braided tensor Categories[96] appear to be another elegant and unified way to resolve many aforementioned issues once and for all. In fact, the connection between LQG and SF Models and Tensor Categories has been recognized for about decades[97, 98, 99]. Note that the string-net condensate due to Wen *et al*[100, 101] also illuminates that tensor categories may be the language underlying a unification of gravity and matter. Braided tensor categories can unleash our program from embedding by casting both trivalent and 4-valent braids combinatorially[98], which is beyond the context of LQG.

A twist of a strand of a braid can be interpreted as characterizing a non-trivial isomorphism from $U(1)$ to $U(1)$. Nonetheless, the concept of twist can be generalized to any vector spaces, which is how it is defined in braided tensor categories. In this manner, we may view spin network labels as if they represent generalized framing of spin networks other than the $U(1)$ framing we have just studied, such that generalized twists can arise, which may offer a unification of our twists and spin network labels, as well as of internal symmetries and spacetime symmetries.

The end-nodes and external edges of 4-valent braids may exert further constraints on what tensor categories are at our disposal or even motivate new types of tensor categories. Tensor-categorized 4-valent braids and evolution moves may be evaluated by the relevant techniques already defined in theories of tensor category or new techniques adapted to our case.

3.7.2 Relation to Topological Quantum Computing

One should not be surprised to notice that the 4-valence scheme of emergent matter is related to Topological Quantum Computing (TQC). This relation has three facets. Firstly, though seemingly superficial, braids and their algebra are present in both disciplines. A major difference is that each 4-valent braid have two end-nodes and has only three strands, which is not the case in TQC.

Secondly, as aforementioned, being a concept rooted in Quantum Computing/Information and adapted to models of quantum gravity, noiseless subsystems are a key underlying notion of the program of emergent matter. Furthermore, [25, 26] suggest that background independent quantum gravity is a quantum information processing system. On the other hand, in [27, 28, 102] topological quantum phase transitions have proven to give rise to emergent gauge and linearized gravitons.

Thirdly, one of our future directions is to employ tensor categories - in particular braided ribbon categories - to make an elegant reformulation of the 4-valent scheme, while TQC is also naturally described in the language of tensor category[103, 104] and related to framed spin networks[99].

Therefore, it is interesting to study TQC from the viewpoint of quantum gravity and vice versa, which may shed new light on both disciplines. For example, we may interpret each 4-valent braid as representing a process of quantum computation, with an end-node of the braid as a fusion rule of anyons or a quantum gate in TQC. We wonder if the interactions of 4-valent braids can be introduced to TQC to study how two quantum processes can join, how one quantum process can split, and when two sequences of quantum processes can be equivalent. Conversely, TQC may assist to decipher or assign new significances of the conserved quantities of 4-valent braids.

4 A Unified Formalism

Recently in [13] the trivalent nodes were recast into the tetravalent scheme, giving a consistent footing to study which results from each scheme could be transferred over to the other. Here we reproduce the unified definition of Braided Ribbon Networks of valence n (with $n \geq 3$) as follows:

- We begin by considering an n -valent graph embedded in a compact 3 dimensional manifold. We construct a 2-surface from this by replacing each node by a 2-sphere with n punctures (1-sphere boundaries on the 2-sphere), and each edge by a tube which is then attached to each of the nodes that it connects to by connecting the tube to one of the punctures on the 2-sphere corresponding to the node.
- Lastly we add to each tube $n - 1$ curves from one puncture to the other and then continue these curves across the sphere in such a way that each of the n tubes connected to a node shares a curve with each of the other tubes.
- We will freely call the tubes between spheres *edges*, the spheres *nodes* and the curves on the tubes *racing stripes* or less formally *stripes*.
- We will call a Braided Ribbon Network the equivalence class of smooth deformations of such an embedding that do not involve intersections of the edges or the racing stripes.

We immediately face the following consequence: under this definition there are only braided ribbon networks of valence 2,3 or 4 (with valence 2 being a collection of framed loops). To see this fact we consider a 5-valent node - a 2-sphere with 5 punctures, with each puncture connected to each other puncture by a non-intersecting curve. Taking each puncture as a node, and the curves as edges, we then get that these objects would constitute the complete graph on 5 nodes and as they lie in the surface of a 2-sphere, such a graph would have to be planar. This is impossible by Kuratowski's theorem[105]: the complete graph on 5 nodes is non-planar. Likewise, we have for any higher valence n that the graph that would be constructed would have the complete graph on 5 nodes as a subgraph, and so they too can not be planar. If the reader desires an intuition for this, it may be instructive to recall that these statements follow from the four colour theorem - the existence of such a node would imply the existence of a map requiring five (or more) colours.

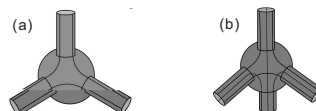


Figure 25: (a) Trivalent node. (b) Four-valent node

We can also introduce a modification to the framework that allows for higher valence vertices. To do this we first make a few definitions.

Definition 4.1. We define the **natural valence** of a braided ribbon network to be the number of racing stripes on each edge.

Definition 4.2. We say that a node is **natural** if each of the tubes which intersect share a racing stripe with each of the other tubes. Otherwise we will say that a node is **composite**.

We can then define a n -valent BRN with natural valence m (here n can take values of $n = km - 2(k - 1)$ for any integer k) as a braided ribbon network where each of the nodes has n tubes which intersect it but where each of the tubes has $m - 1$ racing stripes. Likewise we can define a multi-valent BRN with natural valence m in a similar manner but without fixing the value of k for all nodes. We then construct composite nodes by connecting natural nodes in series by simple edges and shortening the edges which connect them internally until all of these nodes combine into a single sphere with the appropriate number of punctures (see figure 26). As these combined nodes are simply glued they are then dual to gluings of simplices which when grouped together would be equivalent to a polygon (for a natural valence of 3) or a polyhedron with triangular faces (for natural valence of 4).

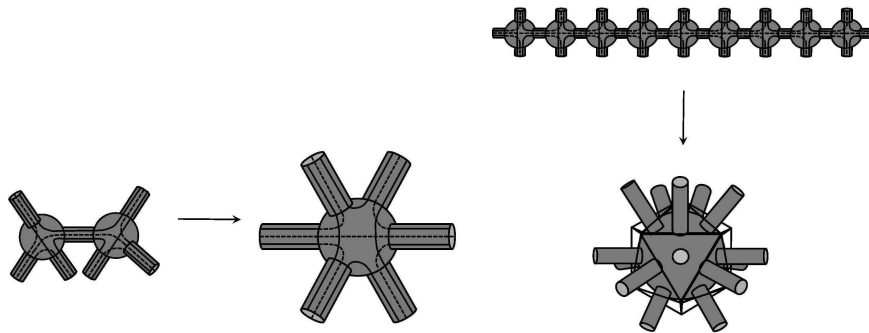


Figure 26: Forming Composite nodes

4.1 Relating to the Ribbon pictures

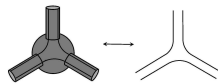


Figure 27: From BRN to trinions

We can construct from the previous form of trivalent braided ribbon graphs a braided ribbon network as we've now defined them as follows: for each node of the network we consider a closed ball in the embedding space which has the node on its surface but which has an empty intersection with the rest of the ribbon graph. These spheres then define the nodes of the braided ribbon network. The edges of the braided ribbon networks are then defined by similarly constructing tubes between these spheres so that the boundaries of the edges of the ribbon graph coincide with the boundary of the tubes. The boundaries of the surface of the ribbon graph then become the racing stripes of the braided ribbon network.

Likewise we can construct a traditional braided ribbon network from a 3-valent braided ribbon network by making the following observation: at each node the racing stripes divide the sphere into two parts, likewise along each edge the tube is divided in two by the racing stripes. We can consistently choose one side or the other and identify this as the surface of a traditional braided ribbon network (alternatively we can think of 'squishing' the two halves together into a single surface, in a sort defining one side to be the 'front' and the other the 'back').

4.2 Applications of the Unified Formalism

In [13] and [14] this formalism was used to demonstrate several general results for Braided Ribbon Networks and embedded spin networks. We shall not reproduce these results here, but instead direct the reader to those papers for demonstrations of:

- The generalization of the reduced link to the unified formalism, and hence to 4-valent BRNs.
- The demonstration of the conservation of the 4-valent reduced link.
- The Construction of maps between BRNs and Spin Networks.
- The demonstration that the reduced link is a conserved quantity for Spin Networks.

These results give us a new use for Braided Ribbon Networks: they have become an effective tool for understanding the information in the embedding of Spin Networks. They also demonstrate that a great deal of the structures that we study in BRNs also exist and are conserved in embedded spin networks.

4.3 Correspondence between the trivalent and tetravalent cases

The natural formulation of framed tetravalent networks, as mentioned in section 3.1, is as tubular links between spherical nodes. It is in fact quite easy to see that such a network can be matched up to a framed trivalent (ribbon) network, by simply “slicing” a tubular link down opposite sides, as discussed in section 4.1

Given any framed trivalent network, we can always combine adjacent nodes to create composite tetravalent nodes. Likewise, the tetravalent nodes of the ribbon networks obtained by the splitting process described above can be decomposed into pairs of trivalent nodes. This allows us to switch between braids in the framed trivalent and tetravalent cases.

Suppose we begin with a trivalent framed braid. We are always able to reduce this braid to its pure twist form, as noted above. Once in this form, in which all crossings have been removed, it is always possible to rotate the node at the top of the braid in such a manner that all the twisting on one strand (say, the rightmost strand) is removed, and extra twists and crossings are induced on the other two strands. We thereby arrive at a braid on three strands in which a single strand does not carry any twisting or crossing. The node at the bottom of this strand may then be freely combined with the node at the top of the braid to form a single tetravalent node. Likewise the nodes at the bottom of the two twisted strands may be combined to form a single tetravalent node. This process is illustrated in Fig. 28. By this process we obtain a braid located between two tetravalent nodes, just as occur in the framed tetravalent case (section 3.1). The braid obtained is, of course, embedded in a ribbon network, but it can always be used to reconstruct a tube-and-sphere framed tetravalent BRN.

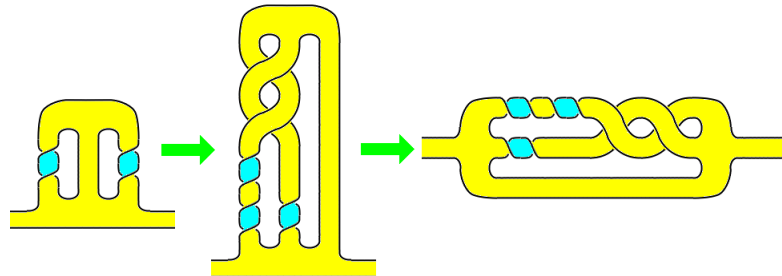


Figure 28: Forming composite nodes allows us to convert between trivalent and tetravalent style braids.

The significance of this construction is that it allows us to associate framed tetravalent networks with structures occurring in the Helon Model (and hence with SM fermions), and allows the structures in the Helon Model to interact via the results on framed tetravalent networks [6]. We thereby obtain a model which allows us to reproduce both kinematic and dynamical aspects of the Standard Model.

5 Conclusions

While the idea of matter emerging from spacetime as topological substructures is an old one, it is only recently that our understanding of the subatomic structure of matter has made models of such emergent matter viable. In this review article we have discussed two parallel approaches, the trivalent and tetravalent scheme, which grew out of the suggestion that the most basic level of substructure within matter may be modelled by braided ribbons. The tetravalent scheme has proven to embody a rich dynamical theory of braid interactions and propagation ruled by topological conservation laws, but has until now not been able to construct a direct mapping to the particle states of the SM, instead producing a seemingly infinite range of equivalence classes of braid states that fall into two types respectively analogous to bosons and fermions. The trivalent scheme has been unable to model interactions, but has been quite successful at taming the profusion of braid states present by constructing equivalence classes of braids, each

equivalence class being mapped to a single type of particle. The unification of trivalent and tetravalent approaches we suggest here promises to allow the development of a fully dynamical theory of interacting particles, to restrict the range of particle states existing within the theory, and to provide a Rosetta stone that allows trivalent braids, tetravalent braids, and the particles of the SM to be equated in a satisfying manner. If successful, this will be a compelling theory of quantum spacetime and emergent matter.

Acknowledgements

SBT is grateful to the Ramsay family for their support through the Ramsay Postdoctoral Fellowship. JH is grateful to his Thesis Advisor Lee Smolin for his discussion and critical comments. YW is in debt to his Supervisor Mikio Nakahara for his constant support and generosity. YW is also supported by “Open Research Center” Project for Private Universities: matching fund subsidy from MEXT, Japan.

References

- [1] S. Bilson-Thompson, arXiv:hep-ph/0503213.
- [2] S. Bilson-Thompson, F. Markopoulou and L. Smolin, *Class. Quant. Grav.* 24 (2007) 3975, arXiv:hep-th/0603022.
- [3] J. Hackett, *Locality and Translations in Braided Ribbon Networks*, *Class. Quant. Grav.* 24 (2007) 5757, arXiv:hep-th/0702198.
- [4] S. Bilson-Thompson, J. Hackett and L. Kauffman, arXiv:0804.0037.
- [5] Y. Wan, arXiv:0710.1312.
- [6] L. Smolin and Y. Wan, *Nucl. Phys.* B796 (2008) 331, arXiv:0710.1548.
- [7] J. Hackett and Y. Wan, *Class. Quant. Grav.* 26 (2009) 125008, arXiv:0803.3203.
- [8] S. He and Y. Wan, *Nucl. Phys.* B804 (2008), arXiv:0805.0453.
- [9] S. He and Y. Wan, *Nucl. Phys.* B805 (2008) 1, arXiv:0805.1265.
- [10] Y. Wan, *Nucl. Phys.* B814 (2009) 1, arXiv:0809.4464.
- [11] F. Markopoulou and I. Prémont-Schwarz, *Class. Quant. Grav.* 25 (2008) 5015, arXiv:0805.3175.
- [12] Bilson-Thompson S., Hackett, J., and Kauffman, L. Particle Topology, Braids, and Braided Belts, *J. Math. Phys.* 50, (2009), 113505, arXiv:0903.1376.
- [13] Hackett J., Invariants of Spin Networks from Braided Ribbon, arXiv:1006.5095.
- [14] Hackett J., Invariants of Braided Ribbon Networks, arXiv:1006.5096.
- [15] H. Harari, *Phys. Lett.* B86 (1979) 83.
- [16] M. Shupe, *Phys. Lett.* B86 (1979) 87.
- [17] Y. Wan, *Emergent Matter of Quantum Geometry*, Ph.D. Thesis, University of Waterloo, 2009.
- [18] W. Thompson (Lord Kelvin), *Proc. Roy. Soc.* Vol. 41, pp. 94–105, Edinburgh, 1867.
- [19] J. A. Wheeler, *Phys. Rev.* 97 (1955) 511.
- [20] D. Finkelstein and C. W. Misner, *Annals of Physics* 6 (1959) 230.
- [21] D. R. Brill and J. B. Hartle, *Phys. Rev.* 135 (1964) B271.
- [22] G. P. Perry and F. I. Cooperstock, *Class. Quant. Grav.* 16 (1999) 1889.
- [23] H. F. Dowker and R. D. Sorkin, *Class. Quant. Grav.* 15 (1998) 1153, arXiv:gr-qc/9609064.
- [24] F. Markopoulou and L. Smolin, *Phys. Rev.* D70 (2004) 124029.
- [25] D. W. Kribs and F. Markopoulou, arXiv:gr-qc/0510052.
- [26] F. Markopoulou, *J. Phys. Conf. Ser.* 67 (2007) 012019, arXiv:gr-qc/0703027.
- [27] M. A. Levin and X. G. Wen, *Rev. Mod. Phys.* 77 (2005) 871, arXiv:cond-mat/0407140.
- [28] Z. C. Gu and X. G. Wen, arXiv:gr-qc/0606100.
- [29] P. Zanardi and M. Rasetti, *Phys. Rev. Lett.* 79 (1997) 3306, arXiv:quant-ph/9705044.
- [30] J. Kempe et al., *Phys. Rev.* A63 (2001) 042307, arXiv:quant-ph/0004064.

-
- [31] J. A. Holbrook, D. W. Kribs and R. Laflamme, *Quant. Inf. Proc.* 2 (2004) 381, arXiv:quant-ph/0402056.
- [32] D. W. Kribs, R. Laflamme and D. Poulin, *Phys. Rev. Lett.* 94 (2005) 180501, arXiv:quant-ph/0412076.
- [33] F. Markopoulou and D. Poulin, Noiseless subsystems and the low energy limit of spin foam models, *Unpublished*.
- [34] O. Dreyer, F. Markopoulou and L. Smolin, *Nucl. Phys.* B744 (2006) 1.
- [35] H. Sahlmann and T. Thiemann, *Class. Quant. Grav.* 23 (2006) 867, arXiv:gr-qc/0207030.
- [36] A. Ashtekar, L. Bombelli and A. Corichi, *Phys. Rev. D* 72 (2005) 02500, arXiv:gr-qc/0504052.
- [37] B. Bahr and T. Thiemann, *Class. Quant. Grav.* 26 (2009) 045011, arXiv:0709.4619.
- [38] T. Thiemann, (Cambridge University Press, 2007).
- [39] E. Alesci and C. Rovelli, *Phys. Rev. D* 76 (2007) 104012, arXiv:0708.0883.
- [40] E. Alesci and C. Rovelli, *Phys. Rev. D* 77 (2008) 044024, arXiv:0711.1284.
- [41] C. Perini, C. Rovelli and S. Speziale, arXiv:0810.1714.
- [42] E. Alesci, E. Bianchi and C. Rovelli, arXiv:0812.5018.
- [43] J. D. Christensen, E. R. Livine and S. Speziale, *Phys. Lett.* B670 (2009) 403, arXiv:0710.0617.
- [44] R. Penrose, *Angular momentum: an approach to combinatorial spacetime* (Cambridge University Press, 1971) .
- [45] R. Penrose, *On the nature of quantum geometry* (Freeman, San Francisco, 1972) .
- [46] C. Rovelli and L. Smolin, *Phys. Rev. D* 52 (1995) 5743, arXiv:gr-qc/9505006.
- [47] J. Kogut and L. Susskind, *Phys. Rev. D* 11 (1975) 395.
- [48] W. Furmanski and A. Kowala, *Nucl. Phys.* B291 (1987) 594.
- [49] J. Wade Cherrington, arXiv:0810.0546.
- [50] J. Wade Cherrington and J. D. Christensen, *Nucl. Phys.* B813 (2009) 370.
- [51] H. Ooguri, *Mod. Phys. Lett.* A7 (1992) 2799.
- [52] V. Turaev and O. Viro, *Topology* 31 (1992) 865.
- [53] L. Crane and I. B. Frenkel, *J. Math. Phys.* 35 (1994) 5136.
- [54] T. J. Foxon, *Class. Quant. Grav.* 12 (1995) 951.
- [55] C. Rovelli, *Quantum Gravity* (Cambridge University Press, 2004).
- [56] J. P. Moussouris, *Quantum models as spacetime based on recoupling theory*, PhD thesis, Oxford, 1983.
- [57] A. Ashtekar, *Lectures on Non-Perturbative Canonical Gravity* (World Scientific, 1991).
- [58] J. C. Baez, *Gauge Fields, Knots and Gravity* (World Scientific, 1994).
- [59] L. Smolin, arXiv:hep-th/0507235.
- [60] L. Smolin, (2007), hep-th/0408048.
- [61] L. Smolin, *Generic Predictions of Quantum Theories of Gravity* (Cambridge University Press, 2009) , arXiv:hep-th/0605052.
- [62] C. Rovelli, *Living Rev. Rel.* 11 (2008) 5.
- [63] R. Loll, *Phys. Rev. Lett.* 75 (1995) 3048.
- [64] R. De Pietri and R. Rovelli, arXiv:gr-qc/9602023.
- [65] F. Markopoulou, arXiv:gr-qc/9704013.
- [66] T. Thiemann, *Phys. Lett. B* 380 (1996) 257, gr-qc/9606088.
- [67] T. Thiemann, *Class. Quant. Grav.* 15 (1998) 839, gr-qc/9606089.
- [68] T. Thiemann, *Class. Quant. Grav.* 15 (1998) 875, gr-qc/9606090.
- [69] J.W. Barrett and L. Crane, *J. Math. Phys.* 39 (1998) 3296, gr-qc/9709028.
- [70] L. Freidel and K. Krasnov, *Class. Quant. Grav.* 25 (2008) 125018, 0708.1595.
- [71] Y. Wan and J. Hackett, *J. Phys. Conf. Ser.* 306 (2011) 012053, arXiv:0811.2161.
- [72] J. C. Baez, *Class. Quant. Grav.* 15 (1998) 1827, arXiv:gr-qc/9709052.
- [73] C. Rovelli, *Living Rev. Rel.* 1 (1998) 1, arXiv:gr-qc/9710008.
- [74] J. C. Baez, *Lect. Notes Phys.* 543 (2000) 25, arXiv:gr-qc/9905087.

-
- [75] U. Pachner, *Ahb. Math. Sem. Univ. Hamburg* 57 (1987) 69.
- [76] R. De Pietri and C. Petronio, *J. Math. Phys.* 41 (2000) 6671, arXiv:gr-qc/0004045.
- [77] S. Major and L. Smolin, *B473* (1996) 267, arXiv:gr-qc/9512020.
- [78] R. Borisssov, S. Major and L. Smolin, *Class. Quant. Grav.* 13 (1996) 3183, arXiv:gr-qc/9512043.
- [79] S. Major, Q-Quantum Gravity, PhD thesis, The Pennsylvania State University, 1997.
- [80] L. Smolin, arXiv:hep-th/0209079.
- [81] P. Ehrenfest, *Proceedings of the Amsterdam Academy* 20 (1917) 200.
- [82] K. Reidemeister, *Knot Theory* (Chelsea, New York, 1948).
- [83] Y. Wan, arXiv:hep-th/0512210.
- [84] B. Dittrich and T. Thiemann, *J. Math. Phys.* 50 (2009) 012503, arXiv:0708.1721.
- [85] C. Rovelli, arXiv:0708.2481.
- [86] C. Rovelli and L. Smolin, *Nucl. Phys.* B442 (1995) 593.
- [87] A. Hamma et al., *Phys. Rev. Lett.* 102 (2009) 017204, 0808.2495.
- [88] E. H. Lieb and D. W. Robinson, *Commun. Math. Phys.* 28 (1972) 251.
- [89] T. Konopka, F. Markopoulou and L. Smolin, (2006), hep-th/0611197.
- [90] T. Konopka, F. Markopoulou and S. Severini, *Phys. Rev.* D77 (2008) 104029, 0801.0861.
- [91] D. Boulatov, *Mod. Phys. Lett. A* 7 (1992) 1629, hep-th/9202074.
- [92] L. Freidel, *Int. J. Theor. Phys.* 44 (2005) 1769, hep-th/0505016.
- [93] D. Oriti, (2006), gr-qc/0512103.
- [94] D. Oriti, arXiv:gr-qc/060703.
- [95] D. Oriti, Spin Foam Models of Quantum Spacetime, PhD thesis, arXiv:gr-qc/0311066.
- [96] C. Kassel, *Quantum Groups Graduate Texts in Mathematics* (Springer Verlag, 1995).
- [97] L. Crane, *Commun. Math. Phys.* 135 (1991) 615.
- [98] Kauffman, Louis H., Map Coloring, q-Deformed Spin Networks, and Turaev-Viro Invariants for 3-Manifolds. *Intl. J. Mod. Phys.* **B(6)**, Nos. 11, 12 (1992), 30 pages.
- [99] Kauffman, Louis H. and Lomonaco, Samuel J., Jr., q-deformed spin networks, knot polynomials and anyonic topological quantum computation, *J. Knot Theory Ramifications*, **16** 3, (2007), 65 pages.
- [100] Z. C. Gu, M. A. Levin and X. G. Wen, *Phys. Rev.* B78 (2008) 205116, arXiv:0807.2010.
- [101] Z. C. Gu et al., *Phys. Rev.* B79 (2009) 085118, arXiv:0809.2821.
- [102] M. A. Levin and X. G. Wen, *Phys. Rev.* B71 (2005) 045110.
- [103] Z. Wang, arXiv:cond-mat/0601285.
- [104] E. C. Rowell, arXiv:0803.1258.
- [105] Kuratowski, K., Sur le problème des courbes gauches en topologie, *Fund. Math.*, **15** (2005), 13 pages.